SNA becomes smaller as the frequency of SNA discharge increases. Future studies are needed to investigate the relation of muscle SNA with other SNAs at faster SNA rhythms, including a cardiac-related SNA rhythm at a frequency of 2 to 6 Hz [36] and an SNA rhythm of 10 Hz [37].

In conclusion, 1-Hz muscle SNA correlated with both renal and cardiac SNAs in time-domain analysis and cohered with renal and cardiac SNAs in frequency-domain analysis. Accompanying an increase in the magnitude of baroreceptor pressure change, both the correlation coefficient and the coherence function increased. These results indicate that muscle SNA correlates and coheres approximately with renal and cardiac SNAs under the closed-loop baroreflex condition and that the arterial baroreflex is capable of potently homogenizing neural discharges of these SNAs by modulating SNA at nonpeak frequencies of SNA autospectra.

APPENDIX

When y is scatter-plotted against x, a linear regression line can be drawn between the two variables. The Pearson product-moment correlation coefficient (r) between variables has the following relationship with variance (Eq. 1) [19]

$$r^2 = 1 - \frac{SS_{res}}{V_y} \quad (1)$$

where SS_{res} is the sum of squared deviations (residuals) from the regression line and V_y is the total sum of squared deviations from the mean of the dependent variable (y), that is, the total variance of y.

Equation 1 indicates that the square of correlation coefficient, r^2, is a fraction of the total variance in the dependent variable (y), which is explained by a linear regression relation [18, 19]. Equation 1 leads to the following relations in Eqs. 2 and 3.

$$V_y \cdot r^2 + SS_{res} = V_y \quad (2)$$

$$SS_{res} = V_y \cdot (1 - r^2) \quad (3)$$

$V_y \cdot r^2$ indicates the component of total variance in y that is explained by a linear regression relation (correlative variance in y). SS_{res} indicates the residual component of total variance in y that is not explained by linear regression relation (noncorrelative variance in y).

This study was supported by the Ground-based Research Announcement for Space Utilization project promoted by the Japan Space Forum, the research project promoted by the Ministry of Health, Labour and Welfare in Japan (#H18-nano-ippan-003), and the Grants-in-Aid for Scientific Research promoted by the Ministry of Education, Culture, Sports, Science and Technology in Japan (#18591992).

REFERENCES

1. Rowell LB. Human cardiovascular control. New York: Oxford Univ. Press; 1993.
2. Mano T. Microneurography as a tool to investigate sympathetic nerve responses to environmental stress. Aviakosmicheskaia i Ekologicheskaia Meditsina. 1997;31:8-14.
3. Wallin BG, Eckberg DL. Sympathetic transients caused by abrupt alterations of carotid baroreceptor activity in humans. Am J Physiol. 1982;242:H185-90.
4. Wallin BG, Esler M, Dorward P, Eisenhofer G, Ferrier C, Westerman R, *et al.* Simultaneous measurements of cardiac noradrenaline spillover and sympathetic outflow to skeletal muscle in humans. J Physiol (Lond). 1992;453:45-58.
5. Wallin BG, Thompson JM, Jennings GL, Esler MD. Renal noradrenaline spillover correlates with muscle sympathetic activity in humans. J Physiol (Lond). 1996;491:881-7.
6. Kamiya A, Michikami D, Fu Q, Niimi Y, Iwase S, Mano T, *et al.* Static handgrip exercise modifies arterial baroreflex control of vascular sympathetic outflow in humans. Am J Physiol Regul Integr Comp Physiol. 2001;281:R1134-9.
7. Markel TA, Daley JC, 3rd, Hogeman CS, Herr MD, Khan MH, Gray KS, *et al.* Aging and the exercise pressor reflex in humans. Circulation. 2003;107:675-8.
8. Mitchell JH, Victor RG. Neural control of the cardiovascular system: insights from muscle sympathetic nerve recordings in humans. Med Sci Sports Exerc. 1996;28(10 Suppl):S60-9.
9. Mosqueda-Garcia R, Furlan R, Tank J, Fernandez-Violante R. The elusive pathophysiology of neurally mediated syncope. Circulation. 2000;102:2898-906.
10. Tank J, Schroeder C, Diedrich A, Szczech E, Haertter S, Sharma AM, *et al.* Selective impairment in sympathetic vasomotor control with norepinephrine transporter inhibition. Circulation. 2003;107:2949-54.
11. Kamiya A, Kawada T, Yamamoto K, Michikami D, Ariumi H, Miyamoto T, *et al.* Muscle sympathetic nerve activity averaged over 1 minute parallels renal and cardiac sympathetic nerve activity in response to a forced baroreceptor pressure change. Circulation. 2005;112:384-6.
12. Kamiya A, Kawada T, Yamamoto K, Michikami D, Ariumi H, Miyamoto T, *et al.* Dynamic and static baroreflex control of muscle sympathetic nerve activity (SNA) parallels that of renal and cardiac SNA during physiological change in pressure. Am J Physiol Heart Circ Physiol. 2005;289:H2641-8.
13. Sundlof G, Wallin BG. Human muscle nerve sympathetic activity at rest. Relationship to blood pressure and age. J Physiol (Lond). 1978;274:621-37.
14. Nakamura T, Kawahara K, Kusunoki M, Feng Z. Microneurography in anesthetized rats for the measurement of sympathetic nerve activity in the sciatic nerve. J Neurosci Methods. 2003;131:35-9.
15. Kawada T, Shishido T, Inagaki M, Tatewaki T, Zheng C, Yanagiya Y, *et al.* Differential dynamic baroreflex regulation of cardiac and renal sympathetic nerve activities. Am J Physiol Heart Circ Physiol. 2001;280:H1581-90.
16. Kent BB, Drane JW, Blumenstein B, Manning JW. A mathematical model to assess changes in the baroreceptor reflex. Cardiology. 1972;57:295-310.
17. Marmarelis PZ, Marmarelis VZ. The whilte noise method in system identification. In: Analysis of Physiological Systems. New York: Plenum; 1978. p. 131-221.
18. Bendat JS, Piersol AG. Random data: analysis and measurement procedures. third edition. Canada: A Wiley-Interscience, 2000.
19. Glantz SA. Primer of biostatistics (4th ed.). New York: McGraw-Hill; 1997.
20. Ikeda Y, Kawada T, Sugimachi M, Kawaguchi O, Shishido T, Sato T, *et al.* Neural arc of baroreflex optimizes dynamic pressure regulation in achieving both stability and quickness. Am J Physiol. 1996;271:H882-90.
21. Habler HJ, Bartsch T, Janig W. Two distinct mechanisms generate the respiratory modulation in fibre activity of the rat cervical sympathetic trunk. J Auton Nerv Syst. 1996;61:116-22.
22. Morrison SF. Respiratory modulation of sympathetic nerve activity: effect of MK-801. Am J Physiol. 1996;270:R645-51.
23. Zhong S, Zhou SY, Gebber GL, Barman SM. Coupled oscillators account for the slow rhythms in sympathetic nerve discharge and phrenic nerve activity. Am J Physiol. 1997;272:R1314-24.
24. Iriki M, Dorward P, Korner PI. Baroreflex "resetting" by arterial hypoxia in the renal and cardiac sympathetic nerves of the rabbit. Pflugers Arch. 1977;370:1-7.
25. Hirai T, Musch TI, Morgan DA, Kregel KC, Claassen DE, Pickar JG, *et al.* Differential sympathetic nerve responses to nitric oxide synthase inhibition in anesthetized rats. Am J Physiol. 1995;269:R807-13.
26. Weiss ML, Claassen DE, Hirai T, Kenney MJ. Nonuniform sympathetic nerve responses to intravenous hypertonic saline infusion. J Auton Nerv Syst. 1996;57:109-15.
27. Macefield VG, Rundqvist B, Sverrisdottir YB, Wallin BG, Elam M. Firing properties of single muscle vasoconstrictor neurons in the sympathoexcitation associated with congestive heart failure. Circulation. 1999;100:1708-13.

28. Narkiewicz K, van de Borne PJ, Pesek CA, Dyken ME, Montano N, Somers VK. Selective potentiation of peripheral chemoreflex sensitivity in obstructive sleep apnea. Circulation. 1999;99:1183-9.
29. Kenney MJ, Barman SM, Gebber GL, Zhong S. Differential relationships among discharges of postganglionic sympathetic nerves. Am J Physiol. 1991;260:R1159-67.
30. Kenney MJ. Frequency characteristics of sympathetic nerve discharge in anesthetized rats. Am J Physiol. 1994;267:R830-40.
31. Kenney MJ, Weiss ML, Patel KP, Wang Y, Fels RJ. Paraventricular nucleus bicuculline alters frequency components of sympathetic nerve discharge bursts. Am J Physiol Heart Circ Physiol. 2001;281:H1233-41.
32. Eckberg DL. The human respiratory gate. J Physiol. 2003;548:339-52.
33. Kamiya A, Hayano J, Kawada T, Michikami D, Yamamoto K, Ariumi H, *et al.* Low-frequency oscillation of sympathetic nerve activity decreases during development of tilt-induced syncope preceding sympathetic withdrawal and bradycardia. Am J Physiol Heart Circ Physiol. 2005;289:H1758-69.
34. Furlan R, Porta A, Costa F, Tank J, Baker L, Schiavi R, *et al.* Oscillatory patterns in sympathetic neural discharge and cardiovascular variables during orthostatic stimulus. Circulation. 2000;101:886-92.
35. Van De Borne P, Montano N, Narkiewicz K, Degaute JP, Malliani A, Pagani M, *et al.* Importance of ventilation in modulating interaction between sympathetic drive and cardiovascular variability. Am J Physiol Heart Circ Physiol. 2001;280:H722-9.
36. Barman SM, Gebber GL. "Rapid" rhythmic discharges of sympathetic nerves: sources, mechanisms of generation, and physiological relevance. J Biol Rhythms. 2000;15:365-79.
37. Barman SM, Gebber GL, Zhong S. The 10-Hz rhythm in sympathetic nerve discharge. Am J Physiol. 1992;262:R1006-14.

J. Physiol. Sci. Vol. 56, No. 3; Jun. 2006; pp. 235–245
Online Jul. 7, 2006; **doi:10.2170/physiolsci.RP006006**

Sympathetic Neural Regulation of Heart Rate Is Robust against High Plasma Catecholamines

Toru KAWADA[1], Tadayoshi MIYAMOTO[1,2], Yuichiro MIYOSHI[1], Sayo YAMAGUCHI[1], Yukiko TANABE[1], Atsunori KAMIYA[1], Toshiaki SHISHIDO[1], and Masaru SUGIMACHI[1]

[1]Department of Cardiovascular Dynamics, Advanced Medical Engineering Center, National Cardiovascular Center Research Institute, Osaka, 565-8565 Japan; and [2]Japan Association for the Advancement of Medical Equipment, Tokyo, 113-0033 Japan

Abstract: The sympathetic regulation of heart rate (HR) may be attained by neural and humoral factors. With respect to the humoral factor, plasma noradrenaline (NA) and adrenaline (Adr) can reportedly increase to levels approximately 10 times higher than resting level during severe exercise. Whether such high plasma NA or Adr interfered with the sympathetic neural regulation of HR remained unknown. We estimated the transfer function from cardiac sympathetic nerve stimulation (SNS) to HR in anesthetized and vagotomized rabbits. An intravenous administration of NA (n = 6) at 1 and 10 $\mu g \cdot kg^{-1} \cdot h^{-1}$ increased plasma NA concentration (pg/ml) from a baseline level of 438 ± 117 (mean ± SE) to 974 ± 106 and 6,830 ± 917 ($P < 0.01$), respectively. The dynamic gain (bpm/Hz) of the transfer function did not change significantly (from 7.6 ± 1.2 to 7.5 ± 1.1 and 8.1 ± 1.1), whereas mean HR (in bpm) during SNS slightly increased from 280 ± 24 to 289 ± 22 ($P < 0.01$) and 288 ± 22 ($P < 0.01$). The intravenous administration of Adr (n = 6) at 1 and 10 $\mu g \cdot kg^{-1} \cdot h^{-1}$ increased plasma Adr concentration (pg/ml) from a baseline level of 257 ± 86 to 659 ± 172 and 2,760 ± 590 ($P < 0.01$), respectively. Neither the dynamic gain (from 8.0 ± 0.6 to 8.4 ± 0.8 and 8.2 ± 1.0) nor the mean HR during SNS (from 274 ± 13 to 275 ± 13 and 274 ± 13) changed significantly. In contrast, the intravenous administration of isoproterenol (n = 6) at 10 $\mu g \cdot kg^{-1} \cdot h^{-1}$ significantly increased mean HR during SNS (from 278 ± 11 to 293 ± 9, $P < 0.01$) and blunted the transfer gain value at 0.0078 Hz (from 5.9 ± 1.0 to 1.0 ± 0.4, $P < 0.01$). In conclusion, high plasma NA or Adr hardly affected the dynamic sympathetic neural regulation of HR.

Key words: systems analysis, neuro-humoral interaction, noradrenaline, adrenaline, isoproterenol.

The sympathetic regulation of heart rate (HR) may be attained by neural and humoral factors. One unique feature of the neural regulation, which is in contrast to the humoral regulation, is its quickness. The quickness of regulation may be best quantified by identifying dynamic characteristics of the input-output or stimulus-response relationship of a given system [1, 2]. Although we have identified the dynamic characteristics of the HR regulation by the cardiac sympathetic nerve by using a transfer function analysis [3, 4], we ignored the possible effects of plasma catecholamines on the transfer function. Plasma concentrations of noradrenaline (NA) and adrenaline (Adr) can increase during systemic sympathetic activation. For instance, plasma NA and Adr both increase to approximately 10 times their respective resting levels during severe exercise [5]. They increase to approximately 6 and 20 times, respectively, during acute myocardial infarction [5]. Whether such high plasma NA or Adr interfered with the dynamic sympathetic neural regulation of HR remained unanswered.

Two mutually opposing hypotheses can be put forward regarding interactions between the humoral and neural factors in the sympathetic regulation of HR. The activation of presynaptic (or prejunctional) α_2-adrenergic receptors located on the postganglionic sympathetic nerve terminals inhibits NA release [6], which would result in the attenuated HR response to cardiac sympathetic nerve stimulation (SNS). In contrast, the activation of presynaptic (or prejunctional) β_2-adrenergic receptors located on the postganglionic sympathetic nerve terminals facilitates NA release [7], which would result in the augmented HR response to cardiac SNS. Besides these interactions, high plasma NA can increase the cardiac uptake of NA [8], which would modify the HR response to cardiac SNS.

The aim of the present study was to test the hypothesis that high plasma NA or Adr alters the dynamic sympathetic neural regulation of HR. Using anesthetized rabbits, we examined the HR response to random cardiac SNS under the condition of elevated plasma NA or Adr induced by exogenous administration. We also examined the effects of an intravenous administration of a β-adrenergic agonist isoproterenol on the HR response to SNS. The results of

Received on Jun 1, 2006; accepted on Jul 4, 2006; released online on Jul 7, 2006; doi:10.2170/physiolsci.RP006006
Correspondence should be addressed to: Toru Kawada, Department of Cardiovascular Dynamics, Advanced Medical Engineering Center, National Cardiovascular Center Research Institute, 5-7-1 Fujishirodai, Suita, Osaka, 565-8565 Japan. Phone: +81-6-6833-5012 (Ext. 2427), Fax: +81-6-6835-5403, E-mail: torukawa@res.ncvc.go.jp

the present study indicated that high plasma NA or Adr hardly affected the dynamic sympathetic neural regulation of HR in anesthetized rabbits.

MATERIALS AND METHODS

Animal preparation. The animals were cared for in strict accordance with the Guiding Principles for the Care and Use of Animals in the Field of Physiological Sciences approved by the Physiological Society of Japan. Eighteen Japanese white rabbits weighing from 2.4 to 3.2 kg were anesthetized by a mixture of α-chloralose (40 mg/ml) and urethane (250 mg/ml), initiated with a bolus injection of 2 ml/kg and maintained with a continuous administration at 0.5 $ml \cdot kg^{-1} \cdot h^{-1}$. The rabbits were intubated and mechanically ventilated with oxygen-enriched room air. The right cardiac postganglionic sympathetic nerve was identified in the right thoracic cavity and sectioned. Usually, HR dropped immediately after the sectioning of the right cardiac sympathetic nerve, suggesting the importance of the right cardiac sympathetic nerve in determining baseline HR. A pair of platinum electrodes was attached to the cardiac end of the sectioned nerve for stimulation. The nerve and electrodes were secured by silicone glue (Kwik-Sil, World Precision Instruments, Sarasota, FL, USA). The left cardiac sympathetic nerve and other sympathetic branches to the heart were kept intact. The carotid sinus nerves and aortic depressor nerves were sectioned bilaterally to minimize changes in systemic sympathetic activity induced by baroreflexes. The vagal nerves were also sectioned bilaterally to eliminate the vagal effect on the heart. The vagotomy did not change HR significantly at this stage, possibly because of the vagolitic effects of the anesthesia. Arterial pressure (AP) was measured by a micromanometer (Millar Instruments, Houston, TX, USA) inserted into the thoracic aorta from the right femoral artery. HR was measured with a cardiotachometer (AT-601G, Nihon Kohden, Tokyo, Japan). An arterial catheter was inserted into the left femoral artery to sample blood for plasma catecholamine measurements. A double-lumen venous catheter was introduced into the right femoral vein for continuous anesthetic infusion and exogenous catecholamine administration.

Protocols. We quantified the dynamic sympathetic neural regulation of HR by using a transfer function analysis [3, 4]. To estimate the transfer function from cardiac SNS to HR, we dynamically stimulated the right cardiac sympathetic nerve as follows. The pulse duration was set at 2 ms, and the pulse amplitude was adjusted to obtain an HR increase of approximately 50 bpm (beats/min) during a 5-Hz constant stimulation in each animal. The resulting amplitude ranged from 0.8 to 2.0 V among animals. With these settings, the stimulation frequency was randomly assigned at either 0 or 5 Hz every 2 s, according to a binary white noise sequence (see appendix A for additional information). The average stimulation frequency was therefore 2.5 Hz. The input power spectral density of SNS was relatively flat up to 0.25 Hz.

In *Protocol 1* ($n = 6$), physiological saline was infused intravenously at 1 $ml \cdot kg^{-1} \cdot h^{-1}$ for 30 min after the end of surgical preparation (Fig. 1). A 300-μl volume of arterial blood was sampled under control conditions (designated as NA_0 condition) for plasma catecholamine measurements. Following the blood sampling, dynamic SNS was applied for 15 min to estimate the transfer function from SNS to HR. Arterial blood was sampled during the last minute of dynamic SNS under the NA_0 condition. Next, 1-μg/ml NA solution was infused at 1 $\mu g \cdot kg^{-1} \cdot h^{-1}$ (NA_1). Fifteen min after the initiation of NA_1 administration, when AP and HR had reached new steady states, arterial blood sampling and 15-min dynamic SNS were repeated. Third, a 10-μg/ml NA solution was administered at 10 $\mu g \cdot kg^{-1} \cdot h^{-1}$ (NA_{10}). Fifteen min after the initiation of NA_{10} administration, arterial blood sampling and 15-min dynamic SNS were repeated.

In *Protocol 2* ($n = 6$), experimental procedures similar to those in *Protocol 1* were conducted, using the Adr solution instead of the NA solution. The transfer function from SNS to HR was estimated under control condition (designated as Adr_0 condition), as well as during the administration of 1-μg/ml Adr solution at 1 $\mu g \cdot kg^{-1} \cdot h^{-1}$ (Adr_1) and 10-μg/ml Adr solution at 10 $\mu g \cdot kg^{-1} \cdot h^{-1}$ (Adr_{10}).

In *Protocol 3* ($n = 6$), we examined the effects of an intravenous administration of a β-adrenergic agonist isoproterenol on the transfer function from SNS to HR. Using experimental procedures similar to those in *Protocol 1*, we

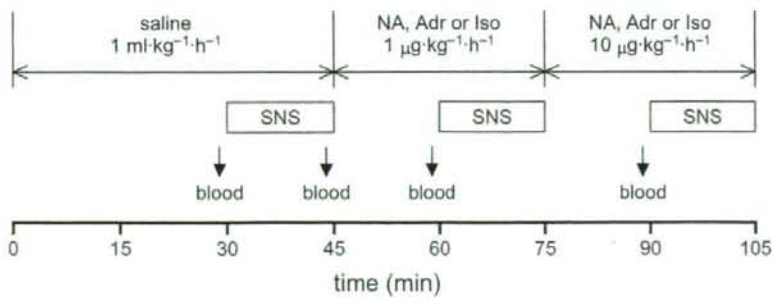

Fig. 1. Schematic diagram showing the experimental protocol. The downward arrows indicate the timings of blood sampling for catecholamine measurements (for *Protocols 1* and *2*). SNS: sympathetic nerve stimulation. NA: noradrenaline; Adr: adrenaline; Iso: isoproterenol.

administered 1-μg/ml isoproterenol solution at 1 $\mu g \cdot kg^{-1} \cdot h^{-1}$ (Iso_1) and 10-μg/ml isoproterenol solution at 10 $\mu g \cdot kg^{-1} \cdot h^{-1}$ (Iso_{10}) and estimated the transfer function under the control (designated as Iso_0), Iso_1, and Iso_{10} conditions.

Data analysis. The SNS command and HR were stored at a sampling rate of 200 Hz. The data were analyzed from only 2 min after the initiation of SNS to remove the initial trend of the HR increase. To estimate the transfer function from SNS to HR, we resampled the SNS-HR data pairs at 8 Hz. These data were segmented into 10 sets of half-overlapping bins of 1,024 data points each. In each segment, a linear trend was subtracted and a Hanning window was applied. The fast Fourier transform was then applied to obtain the frequency spectra of SNS and HR [9]. We calculated the ensemble averages of input power spectral density [$S_{SNS \cdot SNS}(f)$], output power spectral density [$S_{HR \cdot HR}(f)$], and cross-spectral density between the input and output [$S_{HR \cdot SNS}(f)$]. The transfer function [$H(f)$] was estimated using the following equation [10, 11].

$$H(f) = \frac{S_{HR \cdot SNS}(f)}{S_{SNS \cdot SNS}(f)} \tag{1}$$

We also calculated the magnitude-squared coherence function [$Coh(f)$] using the following equation [10, 11].

$$Coh(f) = \frac{|S_{HR \cdot SNS}(f)|^2}{S_{SNS \cdot SNS}(f)\, S_{HR \cdot HR}(f)} \tag{2}$$

The coherence function is a frequency-domain measure of the linear dependence between the input and output signals. A unity coherence value indicates a perfect linear dependence of HR on SNS, whereas a zero coherence value indicates the total independence between SNS and HR.

In *Protocols 1* and *2*, the transfer function from SNS to HR was parameterized by using a mathematical model [$H_m(f)$] of a second-order low-pass filter with pure dead time, using the following equation [3, 12].

$$H_m(f) = \frac{K}{1 + 2\zeta \frac{f}{f_N} j + \left(\frac{f}{f_N} j\right)^2} \exp(-2\pi f\, jL) \tag{3}$$

where K is the dynamic gain (in bpm/Hz), f_N is the natural frequency (in Hz), ζ is the damping ratio, and L is the pure dead time (in s); j represents the imaginary unit (see appendix B for details). A nonlinear iterative least square fitting was performed to minimize the following error function.

$$err = \frac{\sum_{i=1}^{N} |H(f_i) - H_m(f_i)|^2}{\sum_{i=1}^{N} |H(f_i)|^2}, \quad f_i = f_0 \times i \tag{4}$$

where f_0 indicates the fundamental frequency of the Fourier transform. N specifies the upper frequency bound of the fitting procedure. We set N at 32 so as to fit $H_m(f)$ to $H(f)$ up to 0.25 Hz.

In *Protocol 3*, because the transfer function from SNS to HR during Iso_{10} was significantly deviated from the mathematical model of a second-order low-pass filter with pure dead time (Eq. 3), we did not fit the mathematical model to the transfer function and adopted the transfer gain values at the lowest frequency ($G_{0.0078}$) and at 0.1 Hz ($G_{0.1}$) to represent the frequency response of HR to SNS.

Catecholamine measurements. The arterial blood sample was centrifuged and a 100-μl volume of plasma was obtained. The plasma was transferred into a 1.5-ml polypropylene conical tube. A 50-μl volume of the working internal standard solution [100 pg of 3,4-dihydroxybenzylamine (DHBA)], 5 mg of acid-washed alumina, and 1.0 ml of 1-M tris(hydroxymethyl) aminomethane buffer (pH 8.6), containing 0.2% disodium ethylendiaminetetraacetic acid (EDTA), was added to the conical tube and shaken for 15 min. After shaking, the alumina was washed three times with distilled water, transferred into a microfilter (Ultrafree C3, Millipore, Bedford, MA), and centrifuged to remove excess fluid. NA, Adr, and DHBA were then eluted from the alumina, using 60 μl of 2% acetic acid, and their concentrations were measured by using high-performance liquid chromatography with electrochemical detection (DTA-300, Eicom, Kyoto, Japan). Plasma NA and Adr concentrations were calculated, taking into account the recovery rate of DHBA.

Statistical analysis. All data are presented in mean and mean ± SEM values. In *Protocol 1*, the effect of dynamic SNS on the plasma NA concentration was examined by a paired t-test under NA_0 condition. The NA and Adr concentrations before SNS were compared among NA_0, NA_1, and NA_{10} conditions, using Dunnett's test against a single control following the repeated-measures analysis of variance [13]. We also compared mean HR, mean AP, and parameters of the transfer function among NA_0, NA_1, and NA_{10} conditions, using Dunnett's test following repeated-measures analysis of variance. In *Protocol 2*, the effect of dynamic SNS on the plasma Adr concentration was examined by a paired t-test under Adr_0 condition. Other values, including plasma NA and Adr concentrations, mean HR, mean AP, and parameters of the transfer function, were compared among Adr_0, Adr_1, and Adr_{10} conditions, using Dunnett's test following repeated-measures analysis of variance. In *Protocol 3*, mean HR, mean AP, and gain values ($G_{0.0078}$ and $G_{0.1}$) were compared among Iso_0, Iso_1,

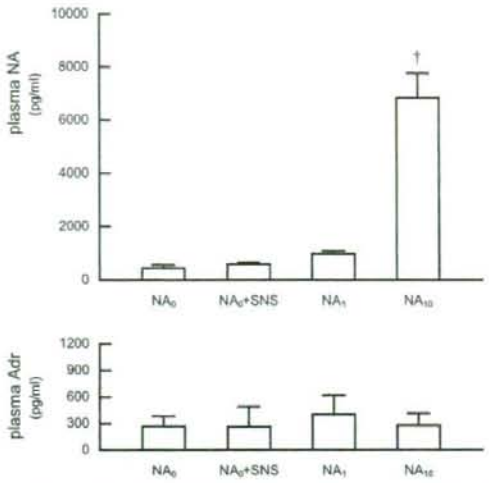

Fig. 2. Plasma concentrations of NA and Adr obtained from *Protocol 1*. The plasma NA concentration was significantly increased during the NA_{10} condition. The plasma Adr concentration was not changed significantly by the NA infusion. NA_0: saline infusion; NA_1 and NA_{10}: noradrenaline infusions at 1 and 10 $\mu g \cdot kg^{-1} \cdot h^{-1}$.

and Iso_{10} conditions, using Dunnett's test following repeated-measures analysis of variance. In all of the statistics, the difference was considered significant at $P < 0.05$.

RESULTS

Effects of high plasma NA on the dynamic sympathetic neural regulation of HR

In *Protocol 1*, dynamic SNS for 15 min did not change the plasma NA or Adr concentration significantly during NA_0 condition (Fig. 2, NA_0 vs. NA_0+SNS). The plasma NA concentration prior to dynamic SNS did not increase significantly during NA_1 condition, but increased to approximately 15 times higher during NA_{10} condition compared to NA_0 condition. The NA infusion did not significantly affect the plasma Adr concentration.

Figure 3A illustrates the time series of SNS, HR, and AP under NA_0, NA_1, and NA_{10} conditions obtained from one animal. The SNS was assigned at 0 or 5 Hz according to a binary white noise sequence. HR changed randomly in response to the dynamic SNS. Mean HR was slightly increased during NA infusion, whereas the amplitude of HR variation appeared unchanged. Mean AP was increased during NA_{10} condition compared to NA_0 condition.

Figure 3B shows averaged transfer functions from SNS to HR during NA_0, NA_1, and NA_{10} conditions obtained from all six animals in *Protocol 1*. The solid curve and the dashed curves in each plot represent mean and mean ± SEM values, respectively. In the gain plot, the transfer

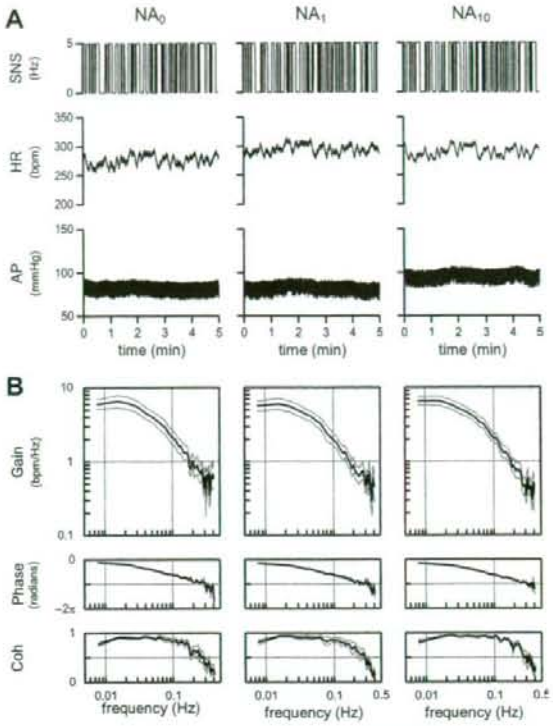

Fig. 3. A: Time series of one animal obtained from *Protocol 1*. Sympathetic nerve stimulation (SNS), heart rate (HR), and arterial pressure (AP) are shown. HR changed dynamically in response to SNS. **B**: Averaged transfer functions from SNS to HR during NA_0, NA_1, and NA_{10} conditions obtained from *Protocol 1* ($n = 6$). NA infusion did not affect the transfer function significantly except for changes in the damping ratio. Solid and dashed curves indicate mean and mean ± SEM values, respectively.

gain decreased with increasing frequency, reflecting the low-pass characteristics of the sympathetic neural regulation of HR. In the phase plot, the phase was near zero radians at the lowest frequency and delayed with increasing frequency, reflecting the SNS increases of HR. In the coherence plot, high coherence values up to 0.2 Hz indicate that approximately 80% of the HR variation in this frequency range was explained by the linear dynamics between SNS and HR. The transfer functions were similar among the three conditions. The dynamic gain, natural frequency, and pure dead time did not differ among the three conditions (Table 1). However, the damping ratio was significantly greater during NA_1 and NA_{10} conditions compared to the NA_0 condition.

Mean HR before SNS did not differ among NA_0, NA_1, and NA_{10} conditions, whereas mean HR during SNS increased significantly during NA_1 and NA_{10} conditions compared to NA_0 condition (Table 1). Although the repeated-measures analysis of variance indicated that the ef-

Table 1. Parameters obtained from *Protocol 1*.

	NA_0	NA_1	NA_{10}
HR, bpm			
Before SNS	248 ± 20	250 ± 19	251 ± 20
During SNS	280 ± 24	289 ± 22**	288 ± 22**
AP, mmHg			
Before SNS	95.7 ± 7.2	99.3 ± 8.1	106.6 ± 6.6*
During SNS	93.6 ± 8.0	102.9 ± 8.8**	106.0 ± 7.0**
Dynamic gain (K), bpm/Hz	7.6 ± 1.2	7.5 ± 1.1	8.1 ± 1.1
Natural frequency (f_N), Hz	0.080 ± 0.010	0.084 ± 0.010	0.083 ± 0.010
Damping ratio (ζ)	1.16 ± 0.05	1.48 ± 0.03*	1.52 ± 0.11*
Pure dead time (L), s	0.44 ± 0.08	0.55 ± 0.07	0.52 ± 0.06
Fitting error (err), %	1.6 ± 0.3	2.2 ± 0.6	1.6 ± 0.4

Values are means ± SEM. **$P < 0.01$ and *$P < 0.05$ vs. the corresponding value obtained during NA_0 condition. HR: heart rate. AP: arterial pressure. SNS: sympathetic nerve stimulation.

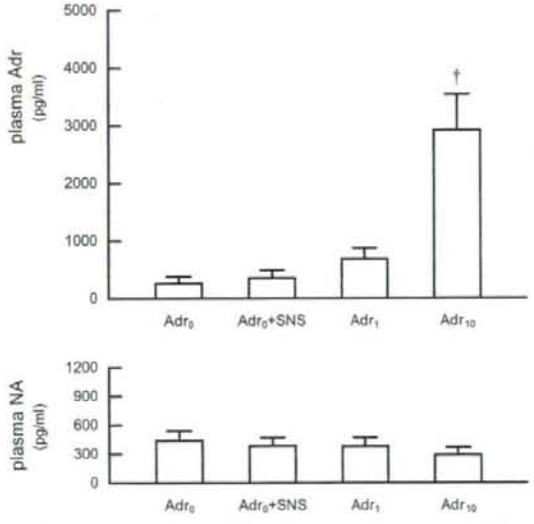

Fig. 4. Plasma concentrations of Adr and NA obtained from *Protocol 2*. The plasma Adr concentration was significantly increased during the Adr_{10} condition. The plasma NA concentration was not changed significantly by Adr infusion. Adr_0: saline infusion; Adr_1 and Adr_{10}: adrenaline infusions at 1 and 10 μg·kg⁻¹·h⁻¹.

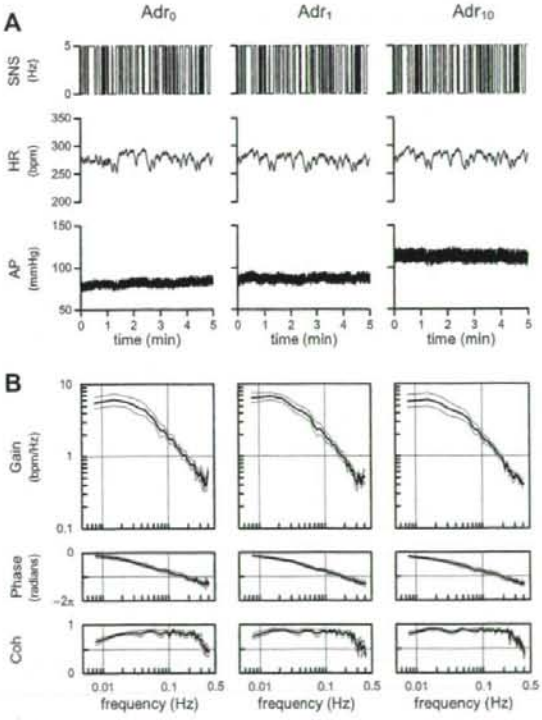

Fig. 5. A: Time series of one animal obtained from *Protocol 2*. HR changed dynamically in response to SNS. **B**: Averaged transfer functions from SNS to HR during Adr_0, Adr_1, and Adr_{10} conditions obtained from *Protocol 2* ($n = 6$). Adr infusion did not affect the transfer function significantly. Solid and dashed curves indicate mean and mean ± SEM values, respectively.

fects of NA infusion on mean HR during SNS were significant, the magnitude of the HR increase was small relative to the interindividual variation of HR. Mean AP before SNS was significantly elevated during NA_{10} condition, but not during NA_1 condition compared to NA_0 condition. Mean AP during SNS was increased significantly during both NA_1 and NA_{10} conditions compared to NA_0 condition.

Table 2. Parameters obtained from *Protocol 2*.

	Adr_0	Adr_1	Adr_{10}
HR, bpm			
Before SNS	231 ± 12	232 ± 10	228 ± 7
During SNS	274 ± 13	275 ± 13	274 ± 13
AP, mmHg			
Before SNS	93.1 ± 9.7	99.0 ± 8.3	113.7 ± 5.2**
During SNS	101.3 ± 8.0	103.8 ± 8.4	116.6 ± 4.6**
Dynamic gain (K), bpm/Hz	8.0 ± 0.6	8.4 ± 0.8	8.2 ± 1.0
Natural frequency (f_N), Hz	0.070 ± 0.005	0.071 ± 0.005	0.067 ± 0.006
Damping ratio (ζ)	1.09 ± 0.20	1.32 ± 0.11	1.39 ± 0.17
Pure dead time (L), s	0.55 ± 0.13	0.66 ± 0.09	0.63 ± 0.15
Fitting error (err), %	2.5 ± 0.5	1.8 ± 0.3	2.3 ± 0.6

Values are means ± SEM. **$P < 0.01$ vs. the corresponding value obtained during Adr_0 condition. HR: heart rate. AP: arterial pressure. SNS: sympathetic nerve stimulation.

Effects of high plasma Adr on the dynamic sympathetic neural regulation of HR

In *Protocol 2*, dynamic SNS for 15 min did not significantly change the plasma Adr or NA concentration during Adr_0 condition (Fig. 4, Adr_0 vs. Adr_0+SNS). The plasma Adr concentration prior to dynamic SNS did not increase significantly during Adr_1 condition, but increased to approximately 11 times higher during Adr_{10} condition compared to Adr_0 condition. The Adr infusion did not significantly affect the plasma NA concentration.

Figure 5A illustrates the time series of SNS, HR, and AP during Adr_0, Adr_1, and Adr_{10} conditions obtained from one animal. HR changed randomly in response to the dynamic SNS. The Adr infusion did not significantly change mean HR or the amplitude of HR variation among Adr_0, Adr_1, and Adr_{10} conditions. Mean AP increased during Adr_{10} condition compared to the Adr_0 condition.

Figure 5B shows averaged transfer functions from SNS to HR during Adr_0, Adr_1, and Adr_{10} conditions obtained from all of the six animals in *Protocol 2*. There seem to be no effects of Adr infusion on the transfer functions. No significant differences in dynamic gain, natural frequency, damping ratio, and pure dead time were observed among the three conditions (Table 2).

Mean HR did not differ significantly among Adr_0, Adr_1, and Adr_{10} conditions, both before and during SNS (Table 2). Mean AP increased significantly during Adr_{10} condition, but not during Adr_1 condition compared with Adr_0 condition, both before and during SNS.

Effects of intravenous isoproterenol on the dynamic sympathetic neural regulation of HR

Figure 6A illustrates the time series of SNS, HR, and AP during Iso_0, Iso_1, and Iso_{10} conditions obtained from one animal. HR changed randomly in response to the dynamic SNS under the Iso_0 condition. Although the dynamic HR response to SNS was maintained under the Iso_1 condition, mean HR was significantly elevated, and no apparent HR response was observed under the Iso_{10} condition.

Figure 6B shows averaged transfer functions from SNS to HR during Iso_0, Iso_1, and Iso_{10} conditions obtained from all of the six animals in *Protocol 3*. The transfer function showed a slight downward shift under the Iso_1 condition compared to the Iso_0 condition. It was significantly deformed and lost consistent characteristics across the animals under the Iso_{10} condition, as evidenced by large standard errors (dashed lines). The gain values ($G_{0.0078}$ and $G_{0.1}$) were significantly lower under the Iso_{10} condition compared to the Iso_0 condition (Table 3).

Mean HR did not change significantly under the Iso_1 condition, but increased significantly under the Iso_{10} condition compared to that under the Iso_0 condition, both before and during SNS (Table 3). Mean AP before SNS was significantly increased under the Iso_1 condition, but not under the Iso_{10} condition compared to that under the Iso_0 condition. Mean AP during SNS did not differ under the Iso_1 condition, but decreased significantly under the Iso_{10} condition compared to that under the Iso_0 condition.

DISCUSSION

We have examined the effects of high plasma NA or Adr on the transfer function from SNS to HR and found that high plasma catecholamines within physiological limits (approximately 10 times the resting levels) were ineffective to alter the sympathetic neural regulation of HR. Although the baseline HR was higher than the resting HR reported in conscious rabbits, the high baseline HR may be partly due to vagotomy. Because dynamic SNS (average stimulation frequency was 2.5 Hz) could increase mean HR, on the average, by 32 bpm in *Protocol 1* and by 43 bpm in *Protocol 2* under control conditions (NA_0 and Adr_0), the insignificant effects of high plasma catecholamines on HR cannot be explained by a simple saturation

Table 3. Parameters obtained from *Protocol 3*.

	Iso_0	Iso_1	Iso_{10}
HR, bpm			
Before SNS	244 ± 7	245 ± 6	289 ± 8**
During SNS	278 ± 11	280 ± 10	293 ± 9**
AP, mmHg			
Before SNS	80.2 ± 8.5	96.2 ± 4.9*	83.5 ± 7.1
During SNS	90.9 ± 7.4	93.1 ± 7.4	82.9 ± 7.0**
$G_{0.0078}$, bpm/Hz	5.9 ± 1.0	4.7 ± 0.8	1.0 ± 0.4**
$G_{0.1}$, bpm/Hz	1.3 ± 0.3	0.9 ± 0.2	0.2 ± 0.2**

Values are means ± SEM. $^{**}P < 0.01$ and $^{*}P < 0.05$ vs. the corresponding value obtained during Iso_0 condition. HR: heart rate. AP: arterial pressure. SNS: sympathetic nerve stimulation. $G_{0.0078}$: transfer gain value at 0.0078 Hz. $G_{0.1}$: transfer gain value at 0.1 Hz.

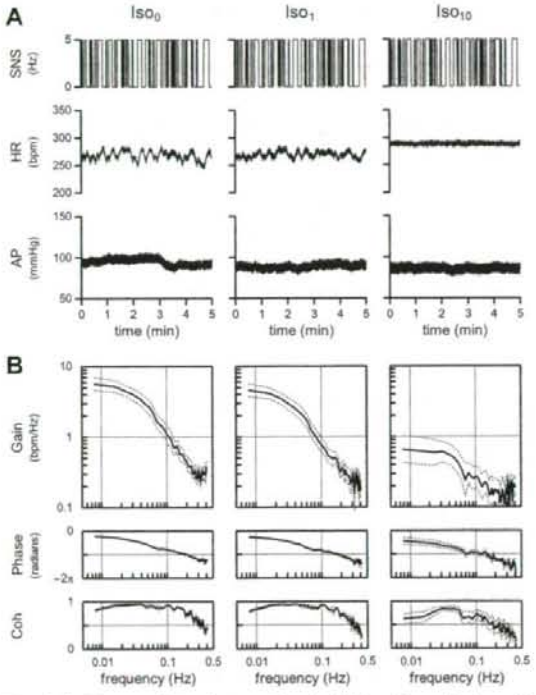

Fig. 6. A: Time series of one animal obtained from *Protocol 3*. Although HR changed dynamically in response to SNS under Iso_0 and Iso_1 conditions, mean HR elevated significantly, and no apparent dynamic HR response was observed under the Iso_{10} condition. **B**: Averaged transfer functions from SNS to HR during Iso_0, Iso_1, and Iso_{10} conditions obtained from *Protocol 3* (n = 6). The transfer gain reduced significantly and varied among animals, as evidenced by the large SEM under the Iso_{10} condition. Solid and dashed curves indicate mean and mean ± SEM values, respectively. Iso_0: saline infusion; Iso_1 and Iso_{10}: isoproterenol infusions at 1 and 10 $\mu g \cdot kg^{-1} \cdot h^{-1}$.

phenomenon of the HR response to catecholamines or by complete downregulation of β-adrenergic receptors under the present experimental settings. Actually, we confirmed that the same dose of intravenous administration of a β-adrenergic agonist isoproterenol increased mean HR significantly and blunted the transfer function (Fig. 6, Iso_{10} in *Protocol 3*). It is quite likely that NA released from the sympathetic nerve terminals during SNS has much stronger effects on HR in comparison with circulating catecholamines.

Effects of high plasma NA on the sympathetic neural regulation of HR

The plasma NA concentration increased approximately 15 times higher during NA_{10} condition than during NA_0 condition. Nevertheless, mean HR before SNS did not change significantly during NA_{10} condition compared to NA_0 condition (Table 1). In contrast, mean AP before SNS increased significantly during NA_{10} condition compared to NA_0 condition (Table 1). Young *et al.* [14] also reported an increase in AP and no changes in HR during NA infusion at 0.2 $\mu g \cdot kg^{-1} \cdot min^{-1}$ (12 $\mu g \cdot kg^{-1} \cdot h^{-1}$) in conscious dogs, though the baroreflexes could have counteracted the potential increase of HR in their study. These results indicate that the vascular bed is more responsive to plasma NA than the sinus node. A tighter synaptic cleft of the neuroeffector junction of the cardiac muscle compared to the vasculature, though it was reported in rat tissues [15], might explain the differential sensitivity to plasma NA between HR and AP.

Cardiac SNS significantly increased the mean HR without increasing the plasma NA concentration (Fig. 2), consistent with previous studies in anesthetized dogs [16] and cats [17]. Although mean HR before SNS did not differ among NA_0, NA_1, and NA_{10} conditions, mean HR during SNS was significantly higher during NA_1 and NA_{10} conditions compared to control (Table 1). These results are in opposition to the hypothesis that high plasma NA activates presynaptic α_2-adrenergic receptors and attenuates the HR response to SNS. One possible explanation for the increased mean HR during SNS under conditions of the NA infusion is as follows. NA released from the sympathetic nerve terminals is removed from the synaptic cleft by two catecholamine uptake mechanisms: a high-affinity, low-capacity neuronal uptake ($uptake_1$) and a low-affinity, high-capacity extraneuronal uptake ($uptake_2$) [5,

18, 19]. The uptake$_1$ mechanism also contributes to plasma clearance of NA [20]. High plasma NA might occupy the uptake$_1$ process to some extent and slow the NA removal from the synaptic cleft during SNS. As a result, the positive chronotropic effects of SNS might be augmented. Honda *et al.* [8] investigated the relationship between the kinetics of plasma catecholamines and cardiac sympathetic nerve activity during systemic hypotension induced by vena cava occlusion. They showed that the cardiac uptake of NA proportionally increased as the arterial NA concentration increased and that there was a negative correlation between the cardiac uptake of NA and the percent increase in mean cardiac sympathetic nerve activity. The negative correlation between the cardiac uptake of NA and the percent increase in mean cardiac sympathetic nerve activity might support the notion that NA of plasma origin and that of neural origin share the uptake$_1$ process. Although the within-individual change was statistically significant, the magnitude of HR increase during SNS was small compared to the interindividual variation of mean HR. Therefore the augmentation of the positive chronotropic effects by high plasma NA may be physiologically insignificant.

In the transfer function parameters, the damping ratio alone was significantly increased during NA_1 and NA_{10} conditions compared with NA_0 condition (Table 1). As already discussed, high plasma NA might have interfered with the uptake$_1$ process and consequently changed the damping ratio of the transfer function [12]. The damping ratio is an important determinant of the system behavior of the second-order low-pass filter. Depending on the value of the damping ratio, the system behaves as underdamped ($0 < \zeta < 1$), critically damped ($\zeta = 1$), or overdamped ($\zeta > 1$) (see appendix B). In the present study, however, the damping ratios changed only from 1.2 to 1.5; thus the system should behave as over-damped under any of the NA_0, NA_1, and NA_{10} conditions. Given that other transfer function parameters including the dynamic gain, natural frequency, and pure dead time did not change significantly, high plasma NA has limited effects on the transfer function from SNS to HR.

Effects of high plasma Adr on the sympathetic neural regulation of HR

The plasma Adr concentration during Adr_{10} condition increased to approximately 11 times that during Adr_0 condition. Although high plasma Adr did not increase HR, it did increase AP (Table 2). In contrast, Young *et al.* [14] reported that an administration of Adr at 0.2 $\mu g \cdot kg^{-1} \cdot min^{-1}$ (12 $\mu g \cdot kg^{-1} \cdot h^{-1}$) significantly increased both AP and HR in conscious dogs. Since the plasma Adr concentration in their study increased to a similar degree to the present result, the HR response to plasma Adr may differ between rabbits and dogs. Other factors that potentially explain the discrepancy are the vagotomy and anesthesia used in the present study. On the other hand, the Adr administration could have altered cardiac sympathetic neural outflow in the study by Young *et al.* [14].

In the present experimental conditions, high plasma Adr did not increase mean HR during SNS compared to Adr_0 condition and did not affect the transfer function from SNS to HR either (Table 2). These results are in opposition to the hypothesis that high plasma Adr activates presynaptic β_2-adrenergic receptors and augments the HR response to SNS. Moreover, because Adr has lower affinity to the uptake$_1$ process compared to NA [18, 19], high plasma NA but not Adr affected the mean HR during SNS and the damping ratio of the transfer function via the mechanism of modulating the NA removal.

The present results are consistent with the study of Boudreau *et al.* [21], in which a 10-min administration of Adr (92 $ng \cdot kg^{-1} \cdot min^{-1}$ or 5.5 $\mu g \cdot kg^{-1} \cdot h^{-1}$) did not increase the NA release in response to cardiac SNS in anesthetized dogs. However, Boudreau *et al.* [21] also demonstrated that a 180-min administration of Adr did increase the NA release in response to cardiac SNS, along with an increased Adr level in the cardiac tissue. Plasma Adr can be taken up into the sympathetic nerve terminals and then coreleased with NA [22]. When Adr is coreleased with NA into the synaptic cleft, NA release may be facilitated via the presynaptic β_2-adrenergic mechanism because Adr is a more potent agonist for β_2-adrenergic receptors than NA [23]. Although the long-term effects of high plasma Adr on the transfer function from SNS to HR was not examined in the present study, it is conceivable that high plasma Adr does not affect the sympathetic neural regulation of HR unless the Adr accumulation in the sympathetic nerve terminals reaches a concentration that is high enough.

Effects of intravenous isoproterenol on the dynamic sympathetic neural regulation of HR

As expected, an intravenous administration of isoproterenol at 10 $\mu g \cdot kg^{-1} \cdot h^{-1}$ increased mean HR significantly both before and during SNS. The transfer gain of the HR response to SNS was significantly decreased under the Iso_{10} condition (Table 3). These results are similar to our previous finding that an increase in mean stimulation frequency of SNS increased mean HR and decreased the transfer gain [12]. We have explained a bidirectional augmentation of the dynamic HR response to autonomic nerve stimulation by using a nonlinear sigmoidal relationship between the autonomic tone and HR [3, 24]. In that concept, the operating point of HR critically affects the transfer gain of the HR response to sympathetic or vagal nerve stimulation; i.e., deviation of the operating point from the center of the sigmoidal relationship decreases the tangential line of the sigmoid curve that relates to the transfer gain. Such operating-point dependence of the transfer gain may explain, at least in part, the decrease in

the transfer gain under the Iso_{10} condition.

Several limitations need to be addressed. First, we performed the experiment in anesthetized rabbits. Because the anesthesia would affect the autonomic tone, the results may not be directly applicable to conscious animals. However, because we cut and stimulated the right cardiac sympathetic nerve, changes in autonomic outflow associated with anesthesia might not have significantly affected the present results. Second, as already mentioned, species differences in HR response to catecholamines may exist. Whether high plasma catecholamines affect the dynamic sympathetic neural regulation of HR in animal species other than rabbits requires further investigations. Third, the duration of catecholamine administration prior to SNS was set at 15 min. Although this priming time was sufficient for AP and HR to reach new steady states, the effects of longer durations of high plasma catecholamines on the dynamic sympathetic neural regulation of HR remain to be investigated. And fourth, because we stimulated the cardiac postganglionic sympathetic nerve, the possible effects of high plasma catecholamines on sympathetic ganglionic transmission were excluded.

In conclusion, although plasma NA or Adr were increased to a level 10–15 times higher than the baseline level by exogenous administration, such high plasma NA or Adr did not significantly affect the dynamic sympathetic neural regulation of HR in anesthetized rabbits. Although humoral and neural factors are thought to regulate the cardiovascular system in concert, the neural factor appears to be much stronger than the humoral factor as far as the HR regulation is concerned.

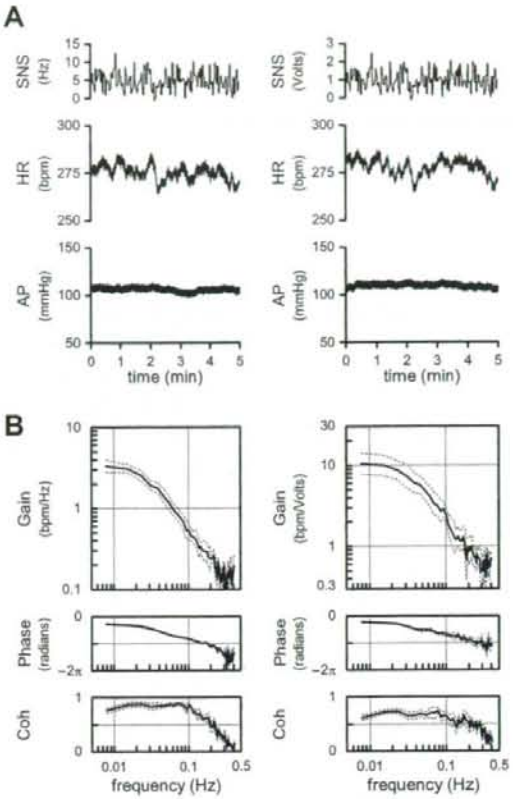

Fig. 7. A: Time series of SNS, HR, and AP using frequency modulation (left) and amplitude modulation (right) as the input signal. HR changed dynamically in response to both the frequency modulation and amplitude modulation of SNS. **B**: Averaged transfer functions obtained from 5 animals using frequency modulation (left) and amplitude modulation (right) as the input signal. Although the absolute gain values are different because of different units in inputs, the low-pass characteristics are in common for both transfer functions.

APPENDIX A

Frequency modulation versus amplitude modulation in nerve stimulation. Because the sinus node responds to NA released from the sympathetic nerve terminals and because the NA kinetics at the neuroeffector junction predominantly determine the low-pass filter characteristics of the HR response to SNS [12], whether the SNS is modulated by frequency or amplitude will not significantly affect the transfer function from SNS to HR. Although the frequency modulation and the amplitude modulation would reveal different nonlinear input-output relationships between the stimulation command signal and the number of nerve fibers actually discharged, a transfer function analysis using a white noise input can retrieve a linear input-output relationship even in the presence of a significant nonlinearity [11]. Although the SNS we used is different from a physiological discharge of nerve fibers, the HR response to physiological nerve discharge would obey the same principle characterized by the transfer function from SNS to HR. When we estimated the transfer function from recorded sympathetic nerve activity to HR, it also approximates to the second-order low-pass filter with pure dead time [25].

We compared the transfer function from SNS to HR identified by the frequency-modulation input and that by the amplitude-modulation input in 5 anesthetized rabbits. The left panel of Fig. 7A shows a typical time series of SNS, HR, and AP obtained from the frequency-modulation input with a constant amplitude of 3 V (2-ms pulse width, 2-s switching interval). The right panel of Fig. 7A shows the time series obtained from the amplitude-modulation input with a constant frequency of 5 Hz (2-ms pulse width, 2-s switching interval). Figure 7B summarizes the averaged transfer function obtained by the frequency-modulation input (left panel) and that by the amplitude-modulation input (right panel). Although the units of gain differ between the two, general low-pass characteristics were in common. The coherence values associated with

the amplitude-modulation input seems smaller than those associated with the frequency-modulation input. In regard to the amplitude-modulation input, the stimulation amplitude usually crosses the threshold amplitude, below which the nerve fibers do not discharge. Such a nonlinear process of the amplitude-modulation input would contribute to the lower coherence values.

APPENDIX B

A mathematical modeling of dynamic heart rate response to sympathetic nerve stimulation using a second-order low-pass filter with pure dead time. We adopted a mathematical model of a second-order low-pass filter with pure dead time to quantify the transfer function from SNS to HR. In the left panel of Fig. 8, the thick line represents a typical transfer function obtained under the NA_0 condition in one animal. The thin smooth curve represents a best-fit mathematical model. A schematic explanation of the model parameters is shown in the right panel of Fig. 8. The dynamic gain, K, determines the value the transfer gain approaches as the frequency goes to zero. The natural frequency, f_N, determines the frequency of low-pass characteristics. The phase of the second-order low-pass filter delays by $\pi/2$ radians at f_N when the pure dead time is zero. The damping ratio, ζ, determines how fast the transfer gain wanes around f_N. As an example, the gain plot shows a slight peaking around f_N when $\zeta = 0.5$. On the other hand, the gain plot shows a more gradual decrease around f_N when $\zeta = 2.0$. The maximum phase delay of the second-order low-pass filter is π radians. The pure dead time, L, determines the additional phase delay necessary for explaining the phase difference between the measured transfer function and the second-order low-pass filter.

This study was supported by "Health and Labour Sciences Research Grant for Research on Advanced Medical Technology" from the Ministry of Health, Labour and Welfare of Japan; "Health and Labour Sciences Research Grant for Research on Medical Devices for Analyzing, Supporting and Substituting the Function of Human Body" from the Ministry of Health, Labour and Welfare of Japan; "Health and Labour Sciences Research Grant H18-Iryo-Ippan-023" from the Ministry of Health, Labour and Welfare of Japan; "Program for Promotion of Fundamental Studies in Health Science" from the National Institute of Biomedical Innovation, a grant provided by the Ichiro Kanehara Foundation; "Ground-based Research Announcement for Space Utilization" promoted by the Japan Space Forum; and "Industrial Technology Research Grant Program in 03A47075" from the New Energy and Industrial Technology Development Organization (NEDO) of Japan.

REFERENCES

1. Kawada T, Fujiki N, Hosomi H. Systems analysis of the carotid sinus baroreflex system using a sum-of-sinusoidal input. Jpn J Physiol. 1992;42:15-34.
2. Kawada T, Yamamoto K, Kamiya A, Ariumi H, Michikami D, Shishido T, Sunagawa K, Sugimachi M. Dynamic characteristics of carotid sinus pressure-nerve activity transduction in rabbits. Jpn J Physiol. 2005;55:157-63.
3. Kawada T, Ikeda Y, Sugimachi M, Shishido T, Kawaguchi O, Yamazaki T, Alexander J Jr, Sunagawa K. Bidirectional augmentation of heart rate regulation by autonomic nervous system in rabbits. Am J Physiol Heart Circ Physiol. 1996;271:H288-95.
4. Kawada T, Sugimachi M, Shishido T, Miyano H, Ikeda Y, Yoshimura R, Sato T, Takaki H, Alexander J Jr, Sunagawa K. Dynamic vagosympathetic interaction augments heart rate response irrespective of stimulation patterns. Am J Physiol Heart Circ Physiol. 1997;272:H2180-7.
5. Cryer PE. Physiology and pathophysiology of the human sympathoadrenal neuroendocrine system. N Eng J Med. 1980;303:436-44.
6. Langer SZ, Adler-Graschinsky E, Giorgi O. Physiological significance of α-adrenoceptor-mediated negative feedback mechanism regulating noradrenaline release during nerve stimulation. Nature. 1977;265:648-50.
7. Majewski H, Rand MJ, Tung LH. Activation of prejunctional β-adrenoceptors in rat atria by adrenaline applied exogenously or released as a co-transmitter. Br J Pharmacol. 1981;73:669-79.
8. Honda T, Ninomiya I, Azumi T. Cardiac sympathetic nerve activity and catecholamine kinetics in cat hearts. Am J Pysiol Heart Circ Physiol. 1987;252:H879-85.
9. Brigham EO. The Fast Fourier Transform and Its Applications. Englewood Cliffs, NJ: Prentice-Hall; 1988. p. 167-203.
10. Bendat JS, Piersol AG. Random Data Analysis and Measurement Procedures. 3rd ed. New York: John Wiley & Sons; 2000. p. 189-217.
11. Marmarelis PZ, Marmarelis VZ. Analysis of Physiological Systems. New York: Plenum; 1978. p. 131-221.
12. Nakahara T, Kawada T, Sugimachi M, Miyano H, Sato T, Shishido T, Yoshimura R, Miyashita H, Inagaki M, Alexander J Jr, Sunagawa K. Neuronal uptake affects dynamic characteristics of heart rate response to sympathetic stimulation. Am J Physiol Regul Integr Comp Physiol. 1999;277:R140-6.
13. Glantz SA. Primer of Biostatistics (5th ed). New York: McGraw-Hill; 2002.
14. Young MA, Hintze TH, Vatner SF. Correlation between cardiac performance and

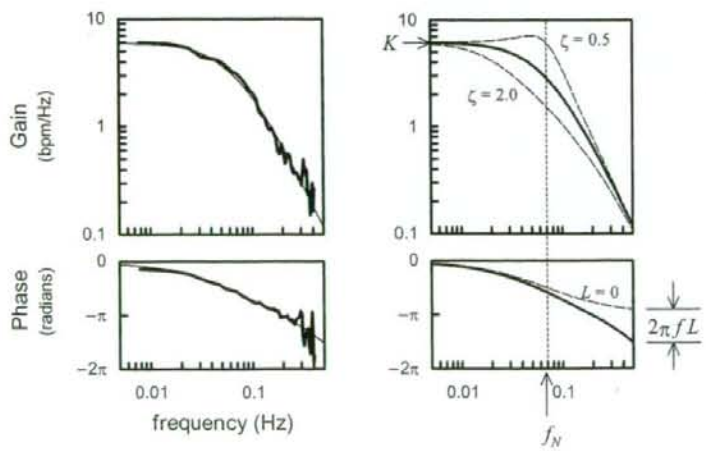

Fig. 8. A: Typical transfer function from SNS to HR obtained under control conditions (NA_0) in one animal. The thin smooth curve is a best-fit mathematical model for the transfer function. **B**: Schematic explanation of the model parameters. K: dynamic gain; f_N: natural frequency; ζ: damping ratio; L: pure dead time.

plasma catecholamine levels in conscious dogs. Am J Physiol Heart Circ Physiol. 1985;248:H82-8.
15. Novi AM. An electron microscope study of the innervation of papillary muscles in the rat. Anat Rec. 1968;160:123-41.
16. Yamaguchi N, de Champlain J, Nadeau R. Correlation between the response of the heart to sympathetic stimulation and the release of endogenous catecholamines into the coronary sinus of the dog. Circ Res. 1975;36:662-8.
17. Kawada T, Yamazaki T, Akiyama T, Shishido T, Miyano H, Sato T, Sugimachi M, Alexander J Jr, Sunagawa K. Interstitial norepinephrine level by cardiac microdialysis correlates with ventricular contractility. Am J Physiol Heart Circ Physiol. 1997;273:H1107-12.
18. Iversen LL. The uptake of catechol amines at high perfusion concentrations in the rat isolated heart: a novel catecholamine uptake process. Brit J Pharmacol. 1965;25:183-33.
19. Iversen LL. Uptake processes for biogenic amines. In: Iversen LL, Iversen SD, Snyder SH, editors. Handbook of Psychopharmacology, Section 1, Vol 3. New York: Plenum Press; 1975. p. 381-442.
20. Friedgen B, Halbrügge T, Graefe K. Role of uptake$_1$ and catechol-O-methyltransferase in removal of circulating catecholamines in the rabbit. Am J Physiol Endocrinol Metab. 1994;267:E814-21.
21. Boudreau G, Péronnet F, de Champlain J, Nadeau R. Presynaptic effects of epinephrine on norepinephrine release from cardiac sympathetic nerves in dogs. Am J Physiol Heart Circ Physiol. 1993;265:H205-11.
22. Esler M, Jennings G, Lambert G, Meredith I, Horne M, Eisenhofer G. Overflow of catecholamine neurotransmitters to the circulation: source, fate, and functions. Physiol Rev. 1990;70:963-85.
23. Schmidt H, Schurr C, Hedler L, Majewski H. Local modulation of norepinephrine release in vivo: Presynaptic β_2-adrenoceptors and endogenous adrenaline. J Cardiovasc Pharmacol. 1984;6:641-9.
24. Kawada T, Sugimachi M, Shidhido T, Miyano H, Sato T, Yoshimura R, Miyashita H, Nakahara T, Alexander J Jr, Sunagawa K. Simultaneous identification of static and dynamic vagosympathetic interactions in regulating heart rate. Am J Physiol Regul Integr Comp Physiol. 1999;276:R782-9.
25. Kawada T, Miyamoto T, Uemura K, Kashihara K, Kamiya K, Sugimachi M, Sunagawa K. Effects of neuronal norepinephrine uptake blockade on baroreflex neural and peripheral arc transfer characteristics. Am J Physiol Regul Integr Comp Physiol. 2004;286:R1110-20.

Am J Physiol Heart Circ Physiol 291: H2187–H2191, 2006.
First published June 9, 2006; doi:10.1152/ajpheart.00175.2006.

Effects of Ca^{2+} channel antagonists on nerve stimulation-induced and ischemia-induced myocardial interstitial acetylcholine release in cats

Toru Kawada,[1] Toji Yamazaki,[2] Tsuyoshi Akiyama,[2] Kazunori Uemura,[1] Atsunori Kamiya,[1] Toshiaki Shishido,[1] Hidezo Mori,[2] and Masaru Sugimachi[1]

[1]*Department of Cardiovascular Dynamics, Advanced Medical Engineering Center, National Cardiovascular Center Research Institute and* [2]*Department of Cardiac Physiology, National Cardiovascular Center Research Institute, Osaka, Japan*

Submitted 17 February 2006; accepted in final form 7 June 2006

Kawada, Toru, Toji Yamazaki, Tsuyoshi Akiyama, Kazunori Uemura, Atsunori Kamiya, Toshiaki Shishido, Hidezo Mori, and Masaru Sugimachi. Effects of Ca^{2+} channel antagonists on nerve stimulation-induced and ischemia-induced myocardial interstitial acetylcholine release in cats. *Am J Physiol Heart Circ Physiol* 291: H2187–H2191, 2006. First published June 9, 2006; doi:10.1152/ajpheart.00175.2006.—Although an axoplasmic Ca^{2+} increase is associated with an exocytotic acetylcholine (ACh) release from the parasympathetic postganglionic nerve endings, the role of voltage-dependent Ca^{2+} channels in ACh release in the mammalian cardiac parasympathetic nerve is not clearly understood. Using a cardiac microdialysis technique, we examined the effects of Ca^{2+} channel antagonists on vagal nerve stimulation- and ischemia-induced myocardial interstitial ACh releases in anesthetized cats. The vagal stimulation-induced ACh release [22.4 nM (SD 10.6), $n = 7$] was significantly attenuated by local administration of an N-type Ca^{2+} channel antagonist ω-conotoxin GVIA [11.7 nM (SD 5.8), $n = 7$, $P = 0.0054$], or a P/Q-type Ca^{2+} channel antagonist ω-conotoxin MVIIC [3.8 nM (SD 2.3), $n = 6$, $P = 0.0002$] but not by local administration of an L-type Ca^{2+} channel antagonist verapamil [23.5 nM (SD 6.0), $n = 5$, $P = 0.758$]. The ischemia-induced myocardial interstitial ACh release [15.0 nM (SD 8.3), $n = 8$] was not attenuated by local administration of the L-, N-, or P/Q-type Ca^{2+} channel antagonists, by inhibition of Na^+/Ca^{2+} exchange, or by blockade of inositol 1,4,5-trisphosphate [$Ins(1,4,5)P_3$] receptor but was significantly suppressed by local administration of gadolinium [2.8 nM (SD 2.6), $n = 6$, $P = 0.0283$]. In conclusion, stimulation-induced ACh release from the cardiac postganglionic nerves depends on the N- and P/Q-type Ca^{2+} channels (with a dominance of P/Q-type) but probably not on the L-type Ca^{2+} channels in cats. In contrast, ischemia-induced ACh release depends on nonselective cation channels or cation-selective stretch activated channels but not on L-, N-, or P/Q type Ca^{2+} channels, Na^+/Ca^{2+} exchange, or $Ins(1,4,5)P_3$ receptor-mediated pathway.

cardiac microdialysis; ω-conotoxin GVIA; ω-conotoxin MVIIC; KB-R7943; verapamil; vagal stimulation

ALTHOUGH N-TYPE Ca^{2+} CHANNELS play a dominant role in norepinephrine release from sympathetic nerve endings (8, 33, 34), the type(s) of Ca^{2+} channels controlling ACh release in the mammalian parasympathetic system is not fully understood and show diversity among reports. To name a few, in isolated parasympathetic submandibular ganglia from the rat, neurotransmission is mediated by Ca^{2+} channels that are resistant to the L-, N-, P/Q-, and R- type Ca^{2+} channel antagonists (29). When the negative inotropic response to field stimulation was examined in the isolated guinea pig atria, Hong and Chang (8) reported the importance of P/Q-type Ca^{2+} channels, whereas Serone et al. (28) reported the importance of N-type Ca^{2+} channels. Because field stimulation in the isolated preparations could induce responses different from those in the in vivo conditions, we aimed to examine the effects of Ca^{2+} channel antagonists on the vagal nerve stimulation-induced myocardial interstitial ACh release in the in vivo feline heart.

Aside from the important role of the normal physiological regulation of the heart, the vagal nerve can be a therapeutic target for certain cardiovascular diseases (2, 3, 13, 22, 27). In previous studies, we have shown that acute myocardial ischemia causes myocardial interstitial ACh release in the ischemic region independently of efferent vagal nerve activity (12, 14). The comparison of the effects of Ca^{2+} channel antagonists on the ACh releases induced by vagal nerve stimulation and by acute myocardial ischemia may deepen our understanding about the ischemia-induced myocardial interstitial ACh release.

A cardiac microdialysis technique offers detailed analyses of in vivo myocardial interstitial ACh release (1, 15). Because the local administration of pharmacological agents through a dialysis probe can modulate ACh release without significantly affecting systemic hemodynamics, a combination of cardiac microdialysis with local pharmacological interventions is useful for analyzing the mechanisms of ACh release in vivo. In the present study, we examined the effects of Ca^{2+} channel antagonists on nerve stimulation- and ischemia-induced ACh releases in anesthetized cats. The results indicate that stimulation-induced ACh release from the cardiac parasympathetic postganglionic nerves depends on the N- and P/Q-type Ca^{2+} channels but probably not on the L-type Ca^{2+} channels. In contrast, ischemia-induced myocardial interstitial ACh release is resistant to the inhibition of L-, N-, and P/Q-type Ca^{2+} channels. In addition, the ischemia-induced myocardial ACh release is resistant to the inhibition of Na^+/Ca^{2+} exchanger and the blockade of inositol 1,4,5-trisphosphate [$Ins(1,4,5)P_3$] receptor but is suppressed by gadolinium, suggesting that nonselective cation channels or cation-selective stretch-activated channels are involved.

MATERIALS AND METHODS

Common Preparation

Animal care was provided in accordance with the *Guiding Principles for the Care and Use of Animals in the Field of Physiological*

Address for reprint requests and other correspondence: T. Kawada, Dept. of Cardiovascular Dynamics, Advanced Medical Engineering Center, National Cardiovascular Center Research Institute, 5-7-1 Fujishirodai, Suita, Osaka 565-8565, Japan (e-mail: torukawa@res.ncvc.go.jp).

The costs of publication of this article were defrayed in part by the payment of page charges. The article must therefore be hereby marked "*advertisement*" in accordance with 18 U.S.C. Section 1734 solely to indicate this fact.

Sciences approved by the Physiological Society of Japan. All protocols were approved by the Animal Subjects Committee of the National Cardiovascular Center. Adult cats weighing from 2.2 to 4.2 kg were anesthetized via an intraperitoneal injection of pentobarbital sodium (30–35 mg/kg) and ventilated mechanically with room air mixed with oxygen. The depth of anesthesia was maintained with a continuous intravenous infusion of pentobarbital sodium (1–2 $mg \cdot kg^{-1} \cdot h^{-1}$) through a catheter inserted from the right femoral vein. Systemic arterial pressure was monitored from a catheter inserted from the right femoral artery. The vagi were sectioned bilaterally at the neck. The esophageal temperature of the animal, which was measured by a thermometer (CTM-303, TERUMO, Japan), was maintained at around 37°C using a heated pad and a lamp.

With the animal in the lateral position, the left fifth and sixth ribs were resected to expose the heart. A dialysis probe was implanted transversely, using a fine guiding needle, into the anterolateral free wall of the left ventricle perfused by the left anterior descending coronary artery (LAD). Heparin sodium (100 U/kg) was administered intravenously to prevent blood coagulation. At the end of the experiment, the experimental animals were killed with an overdose of pentobarbital sodium. Postmortem examination confirmed that the dialysis probe had been threaded in the middle layer of the left ventricular myocardium. The thickness of the left ventricular free wall was ~7–8 mm, and the semipermeable membrane of the dialysis probe was positioned ~3–4 mm from the epicardial surface.

Dialysis Technique

The materials and properties of the dialysis probe have been described previously (1). Briefly, we designed a transverse dialysis probe. A dialysis fiber of semipermeable membrane (13 mm length, 310 μm OD, 200 μm ID; PAN-1200, 50,000 molecular weight cutoff, Asahi Chemical, Japan) was glued at both ends to polyethylene tubes (25 cm length, 500 μm OD, 200 μm ID). The dialysis probe was perfused at a rate of 2 μl/min with Ringer solution containing a cholinesterase inhibitor eserine (physostigmine, 100 μM). Experimental protocols were started 2 h after the dialysis probe was implanted when the ACh concentration in the dialysate reached a steady state. The ACh concentration in the dialysate was measured by high-performance liquid chromatography with electrochemical detection (Eicom, Kyoto, Japan).

Local administration of a pharmacological agent was carried out through a dialysis probe. That is to say, we added the pharmacological agent to the perfusate and allowed 1 h for a settling time. The pharmacological agent should spread around the semipermeable membrane, thereby affecting the neurotransmitter release in the vicinity of the semipermeable membrane. Because the distribution across the semipermeable membrane is required, based on previous results (33, 34), we used the pharmacological agent at the concentration 10–100 times higher than that required for complete channel blockade in experimental settings in vitro.

Specific Preparation and Protocols

Protocol 1. Bipolar platinum electrodes were attached bilaterally to the cardiac ends of the sectioned vagi at the neck. The nerves and electrodes were covered with warmed mineral oil for insulation. The vagal nerves were stimulated for 15 min (20 Hz, 1 ms, 10 V). We measured the stimulation-induced ACh release in the absence of Ca^{2+} channel blockade (control, $n = 7$) and examined the effects of an L-type Ca^{2+} channel antagonist verapamil (100 μM, $n = 5$), an N-type Ca^{2+} channel antagonist ω-conotoxin GVIA (10 μM, $n = 7$), a P/Q-type Ca^{2+} channel antagonist ω-conotoxin MVIIC (10 μM, $n = 6$), and combined administration of ω-conotoxin GVIA and ω-conotoxin MVIIC (10 μM each, $n = 6$).

Protocol 2. Because a preliminary result from *protocol 1* suggested that local administration of verapamil was ineffective in suppressing stimulation-induced ACh release, we examined the effects of the intravenous administration of verapamil (300 μg/kg, $n = 6$) on stimulation-induced ACh release in vagotomized animals as a supplemental experiment.

Protocol 3. A 60-min LAD occlusion was performed by using a 3-0 silk suture passed around the LAD just distal to the first diagonal branch. We measured the ACh levels during 45–60 min of ischemia in the absence of Ca^{2+} channel blockade (control, $n = 8$) and examined the effects of verapamil (100 μM, $n = 5$), ω-conotoxin GVIA (10 μM, $n = 5$), and ω-conotoxin MVIIC (10 μM, $n = 5$). A previous result indicated that the ischemia-induced ACh release reached the steady state during 45–60 min of ischemia (14). We also examined the effects of three additional agents, a Na^+/Ca^{2+} exchange inhibitor KB-R7943 (10 μM, $n = 5$) (9, 10), an $Ins(1,4,5)P_3$ receptor blocker xestospongin C (500 μM, $n = 6$) (25), and a nonselective cation channel blocker or a cation-selective stretch activated channel blocker gadolinium (1 mM) (5, 17), on the ischemia-induced ACh release.

Statistical Analysis

All data are presented as mean (SD) values. In *protocol 1*, we compared stimulation-induced ACh release among the five groups using one-way analysis of variance followed by the Student-Neuman-Keuls test (6). In *protocol 2*, we used an unpaired-*t* test (two-sided) to examine the effect of intravenous verapamil administration on stimulation-induced ACh release. In *protocol 3*, we compared ischemia-induced ACh release among the seven groups using one-way analysis of variance followed by the Dunnett' test against the control. For all analyses, differences were considered significant when $P < 0.05$.

RESULTS

In *protocol 1*, the ACh level during electrical vagal stimulation was 22.4 nM (SD 10.6). Local administration of verapamil did not affect stimulation-induced ACh release (Fig. 1). In contrast, local administration of ω-conotoxin GVIA or ω-conotoxin MVIIC suppressed stimulation-induced ACh release. The extent of suppression was greater in the latter. The ACh level was significantly lower in the simultaneous administration group (ω-conotoxin GVIA + ω-conotoxin MVIIC)

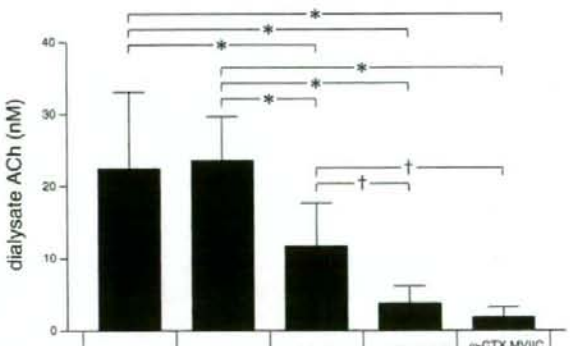

	vehicle	verapamil	ω-CTX GVIA	ω-CTX MVIIC	ω-CTX MVIIC + ω-CTX GVIA
vehicle		0.758	0.0054	0.0002	0.0002
verapamil	0.758		0.0068	0.0002	0.0001
GVIA	0.0054	0.0068		0.033	0.025
MVIIC	0.0002	0.0002	0.033		0.581
MVIIC+GVIA	0.0002	0.0001	0.025	0.581	

Fig. 1. Effects of local administration of verapamil, ω-conotoxin GVIA, ω-conotoxin MVIIC, or ω-conotoxin GVIA plus ω-conotoxin MVIIC on vagal nerve stimulation-induced myocardial interstitial ACh release. Both ω-conotoxin GVIA and ω-conotoxin MVIIC, but not verapamil, suppressed stimulation-induced ACh release. Data are mean (SD) values. *$P < 0.01$, †$P < 0.05$. The exact P values are presented.

than that in the ω-conotoxin GVIA group but was not different from the ω-conotoxin MVIIC group.

In *protocol 2*, the intravenous administration of verapamil did not significantly change stimulation-induced ACh release [21.7 nM (SD 12.8)] compared with the control group ($P = 0.91$).

In *protocol 3*, the ACh level in the ischemic region was 14.9 nM (SD 8.3) during 45–60 min of acute myocardial ischemia. Inhibition of voltage-dependent Ca^{2+} channels by local administration of verapamil, ω-conotoxin GVIA, or ω-conotoxin MVIIC did not affect ischemia-induced ACh release (Fig. 2). Inhibition of the reverse mode action of Na^+/Ca^{2+} exchange by local administration of KB-R7943 appeared to have augmented rather than suppressed ischemia-induced ACh release, though there was no statistically significant difference from the control. Blockade of the $Ins(1,4,5)P_3$ receptor by local administration of xestospongin C did not affect the ischemia-induced ACh release. In contrast, blockade of nonselective cation channels or cation-selective stretch-activated channels by local administration of gadolinium suppressed the ischemia-induced ACh release.

DISCUSSION

Ca^{2+} Channels Involved in Stimulation-Induced ACh Release

Although neurotransmitter release at mammalian sympathetic neuroeffector junctions predominantly depends on Ca^{2+} influx through N-type Ca^{2+} channels (23, 33, 34), the type(s) of Ca^{2+} channels involved in ACh release from cardiac parasympathetic neuroeffector junctions show diversity among reports (8, 28). One possible factor hampering investigations into parasympathetic postganglionic neurotransmitter release in response to vagal nerve stimulation in vivo is that the parasympathetic ganglia are usually situated in the vicinity of the effector organs, thereby making it difficult to separately assess ACh release from preganglionic and postganglionic nerves. In the previous study from our laboratory, intravenous administration, but not local administration of a ganglionic blocker, hexamethonium reduced vagal stimulation-induced ACh release assessed by cardiac microdialysis (1). The negligible effect of local hexamethonium administration on stimulation-induced ACh release suggests the lack of parasympathetic ganglia around the dialysis probe. In support of our speculation, a recent neuroanatomical finding indicates that three ganglia, away from the left anterior free wall targeted by the dialysis probe, provide the major source for left ventricular postganglionic innervation in cats: a cranioventricular ganglion, a left ventricular ganglion 2 (so designated), and an interventriculo-septal ganglion (11). Therefore, ACh, as measured by cardiac microdialysis, is considered to predominantly reflect ACh release from parasympathetic postganglionic nerves.

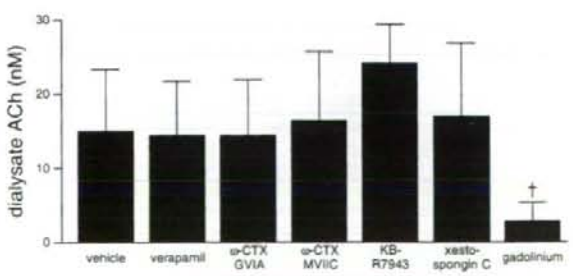

Fig. 2. Effects of local administration of verapamil, ω-conotoxin GVIA, ω-conotoxin MVIIC, KB-R7943, xestospongin C, or gadolinium on acute myocardial ischemia-induced myocardial interstitial ACh release in the ischemic region. Gadolinium alone suppressed the ischemia-induced ACh release. Data are mean (SD) values. †$P < 0.05$. The exact P values are presented.

Local (*protocol 1*) or intravenous (*protocol 2*) administration of verapamil did not affect stimulation-induced ACh release. In contrast, vagal stimulation-induced ACh release was reduced in both the ω-conotoxin GVIA and ω-conotoxin MVIIC groups but to a greater extent in the latter (Fig. 1). Therefore, both N- and P/Q-type, but probably not L-type, Ca^{2+} channels are involved in stimulation-induced ACh release from the cardiac parasympathetic postganglionic nerves in cats. The contribution of P/Q type Ca^{2+} channels to ACh release might be greater than that of N-type Ca^{2+} channels. Hong and Chang (8) reported that the negative inotropic response to field stimulation depends predominantly on the P/Q-type Ca^{2+} channels in isolated guinea pig atria, whereas Serone et al. (28) reported the predominance of N-type Ca^{2+} channels. In those studies, the field stimulation employed differed from ordinary activation of the postganglonic nerves by nerve discharge and, in addition, ACh release was not directly measured. The present study directly demonstrated the involvement of P/Q- and N-type Ca^{2+} channels in the stimulation-induced ACh release in the cardiac parasympathetic postganglionic nerves. These results support the concept that multiple subtypes of the voltage-gated Ca^{2+} channel mediate transmitter release from the same population of parasympathetic neurons (31).

Stimulation-induced ACh release was suppressed by ~50% in the ω-conotoxin GVIA group and by ~80% in the ω-conotoxin MVIIC group. The algebraic summation of the extent of suppression exceeded 100%. The phenomenon may be in part due to the nonlinear dose-response relationship between Ca^{2+} influx and transmitter release (32). The supra-additive phenomenon may be also due to the affinity of ω-conotoxin MVIIC to N-type Ca^{2+} channels (8, 26, 36). Combined local administration of ω-conotoxin GVIA and ω-conotoxin MVIIC almost completely suppressed stimulation-induced ACh release to a level similar to that achieved by the Na^+ channel inhibitor tetrodotoxin (15). Therefore, involvement of another untested type of Ca^{2+} channel(s) is unlikely in the stimulation-induced ACh release from the cardiac parasympathetic postganglionic nerves in cats.

Ca^{2+} Channels and Ischemia-Induced ACh Release

In a previous study, we showed that acute myocardial ischemia evokes myocardial interstitial ACh release in the ischemic region via a local mechanism independent of efferent vagal nerve activity (14). In that study, the inhibition of intracellular Ca^{2+} mobilization by local administration of 3,4,5-trimethoxybenzoic acid 8-(diethyl amino)-octyl ester (TMB-8) suppressed ischemia-induced ACh release, suggesting that an axoplasmic Ca^{2+} elevation is essential for the ischemia-induced ACh release. Because tissue K^+ concentration increases in the ischemic region (7, 18), high K^+-induced

depolarization could activate voltage-dependent Ca^{2+} channels even in the absence of efferent vagal nerve activity. However, ischemia-induced ACh release was not suppressed by local administration of verapamil, ω-conotoxin GVIA, or ω-conotoxin MVIIC (Fig. 2). Therefore, Ca^{2+} entry through the voltage-dependent Ca^{2+} channels is unlikely a mechanism for the ischemia-induced myocardial interstitial ACh release.

Acute myocardial ischemia causes energy depletion in the ischemic region, which impairs Na^+-K^+-ATPase activity. Ischemia also causes acidosis in the ischemic region, which promotes Na^+/H^+ exchange. As a result, ischemia causes intracellular Na^+ accumulation. The decrease in the Na^+ gradient across the plasma membrane may then cause the Na^+/Ca^{2+} exchanger to operate in the reverse mode, facilitating intracellular Ca^{2+} overload. KB-R7943 can inhibit the reverse mode of Na^+/Ca^{2+} exchange (9, 10) and its potential to protect against ischemia-reperfusion injury has been reported (21). In the present study, however, local administration of KB-R7943 failed to suppress and rather increased ACh release during ischemia as opposed to our expectation. It is plausible that the inhibition of reverse mode of Na^+/Ca^{2+} may have facilitated the accumulation of intracellular Na^+ and induced adverse effects that cancelled the possible beneficial effects derived from the inhibition of Ca^{2+} entry through the Na^+/Ca^{2+} exchanger itself. In addition, KB-R7943 could inhibit the forward mode of Na^+/Ca^{2+} exchange and reduce Ca^{2+} efflux (16), contributing to the intracellular Ca^{2+} accumulation and ACh release. In the present study, we observed the effects of KB-R7943 only during the ischemic period. However, accumulation of intracellular Na^+ through Na^+/H^+ exchange is enhanced on reperfusion due to the washout of extracellular H^+ (20). The inhibition of Na^+/Ca^{2+} exchange to suppress Ca^{2+} overload might become more important during the reperfusion phase. For instance, the percent segment shortening of the left ventricle was improved by KB-R7943 during reperfusion but not during ischemia (35).

As already mentioned, the ischemia-induced ACh release can be blocked by TMB-8 and thus the intracellular Ca^{2+} mobilization is required for the ischemia-induced ACh release (14). Besides the Ca^{2+} entries through voltage-dependent Ca^{2+} channels and via the reverse mode of Na^+/Ca^{2+} exchanger, Ca^{2+} may be mobilized from the endoplasmic reticulum via pathological pathways. As an example, the mitochondrial permeability transition pore triggered in pathological conditions is linked to cytochrome *c* release. Cytochrome *c* can bind to the endoplasmic reticulum Ins(1,4,5)P_3 receptor, rendering the channel insensitive to autoinhibition by high cytosolic Ca^{2+} concentration and resulting in enhanced endoplasmic reticulum Ca^{2+} release (4, 30). In the present study, however, blockade of Ins(1,4,5)P_3 receptor by xestospongin C failed to suppress the ischemia-induced ACh release. In contrast, local administration of gadolinium significantly suppressed the ischemia-induced ACh release. Therefore, nonselective cation channels or cation-selective stretch-activated channels contribute to the ischemia-induced ACh release. During myocardial ischemia, the ischemic region can be subjected to paradoxical systolic bulging. Such bulging likely opens stretch-activated channels and causes myocardial interstitial ACh release, possibly leading to cardioprotection by ACh against ischemic injury (2).

Limitations

First, the experiment was performed under anesthetic conditions, which may have influenced basal autonomic activity. However, because we sectioned the vagi at the neck, basal autonomic activity may have had only a minor effect on ACh release during the vagal stimulation and during acute myocardial ischemia. Second, we added eserine to the perfusate to inhibit immediate degradation of ACh (24), which may have increased the ACh level in the synaptic cleft and activated regulatory pathways such as autoinhibition of ACh release via muscarinic receptors (24). However, the myocardial interstitial ACh level measured under this condition could reflect changes induced by Na^+ channel inhibitor, choline uptake inhibitor, and vesicular ACh transport inhibitor as described in a previous study (15). Therefore, we think that the interpretation of the present results is reasonable. Third, tissue and species differences should be taken into account when extrapolating the present findings, because significant heterogeneity in the Ca^{2+} channels involved in the mammalian parasympathetic system may exist. Finally, we used verapamil to test the involvement of L-type Ca^{2+} channels in the ACh release. There are three major types of L-type Ca^{2+} channel antagonists with different binding domains (verapamil, nifedipine, and diltiazem) (19). Whether the effects on the ACh release are common among the three types of L-type Ca^{2+} channel antagonists remains unanswered.

In conclusion, the N- and P/Q-type Ca^{2+} channels (with the P/Q-type dominant), but probably not the L-type Ca^{2+} channels, are involved in vagal stimulation-induced ACh release from the cardiac parasympathetic postganglionic nerves in cats. In contrast, myocardial interstitial ACh release in the ischemic myocardium is resistant to the blockade of L-, N-, and P/Q-type Ca^{2+} channels. In addition, the ischemia-induced myocardial ACh release is resistant to the inhibition of Na^+/Ca^{2+} exchanger and the blockade of Ins(1,4,5)P_3 receptor but is suppressed by gadolinium, suggesting that nonselective cation channels or cation-selective stretch-activated channels are involved.

GRANTS

This study was supported by Health and Labour Sciences Research Grant for Research on Advanced Medical Technology from the Ministry of Health, Labour and Welfare of Japan, Health and Labour Sciences Research Grant for Research on Medical Devices for Analyzing, Supporting and Substituting the Function of Human Body from the Ministry of Health, Labour and Welfare of Japan, Health and Labour Sciences Research Grant H18-Iryo-Ippan-023 from the Ministry of Health, Labour and Welfare of Japan, Program for Promotion of Fundamental Studies in Health Science from the National Institute of Biomedical Innovation, a Grant provided by the Ichiro Kanehara Foundation, Ground-based Research Announcement for Space Utilization promoted by Japan Space Forum, and Industrial Technology Research Grant Program in 03A47075 from New Energy and Industrial Technology Development Organization of Japan.

REFERENCES

1. **Akiyama T, Yamazaki T, and Ninomiya I.** In vivo detection of endogenous acetylcholine release in cat ventricles. *Am J Physiol Heart Circ Physiol* 266: H854–H860, 1994.
2. **Ando M, Katare RG, Kakinuma Y, Zhang D, Yamasaki F, Muramoto K, and Sato T.** Efferent vagal nerve stimulation protects heart against ischemia-induced arrhythmias by preserving connexin43 protein. *Circulation* 112: 164–170, 2005.

3. **Bibevski S and Dunlap ME.** Prevention of diminished parasympathetic control of the heart in experimental heart failure. *Am J Physiol Heart Circ Physiol* 287: H1780–H1785, 2004.
4. **Brookes PS, Yoon Y, Robotham JL, Anders MW, and Sheu SS.** Calcium, ATP, and ROS: a mitochondrial love-hate triangle. *Am J Physiol Cell Physiol* 287: C817–C833, 2004.
5. **Caldwell RA, Clemo HF, and Baumgarten CM.** Using gadolinium to identify stretch-activated channels: technical considerations. *Am J Physiol Cell Physiol* 275: C619–C621, 1998.
6. **Glantz SA.** *Primer of Biostatistics* (5th ed) New York: McGraw-Hill, 2002.
7. **Hirche HJ, Franz CHR, Bös L, Bissig R, Lang R, and Schramm M.** Myocardial extracellular K^+ and H^+ increase and noradrenaline release as possible cause of early arrhythmias following acute coronary artery occlusion in pigs. *J Mol Cell Cardiol* 12: 579–593, 1979.
8. **Hong SJ and Chang CC.** Calcium channel subtypes for the sympathetic and parasympathetic nerves of guinea-pig atria. *Br J Pharmacol* 116: 1577–1582, 1995.
9. **Iwamoto T, Kita S, Uehara A, Inoue Y, Taniguchi Y, Imanaga I, and Shigekawa M.** Structural domains influencing sensitivity to isothiourea derivative inhibitor KB-R7943 in cardiac Na^+/Ca^{2+} exchanger. *Mol Pharmacol* 59: 524–531, 2001.
10. **Iwamoto T, Watano T, and Shigekawa M.** A novel isothiourea derivative selectively inhibits the reverse mode of Na^+/Ca^{2+} exchange in cells expressing NCX1. *J Biol Chem* 271: 22391–22397, 1996.
11. **Johnson TA, Gray AL, Lauenstein JM, Newton SS, and Massari VJ.** Parasympathetic control of the heart. I. An interventriculo-septal ganglion is the major source of the vagal intracardiac innervation of the ventricles. *J Appl Physiol* 96: 2265–2272, 2004.
12. **Kawada T, Yamazaki T, Akiyama T, Inagaki M, Shishido T, Zheng C, Yanagiya Y, Sugimachi M, and Sunagawa K.** Vagosympathetic interactions in ischemia-induced myocardial norepinephrine and acetylcholine release. *Am J Physiol Heart Circ Physiol* 280: H216–H221, 2001.
13. **Kawada T, Yamazaki T, Akiyama T, Li M, Ariumi H, Mori H, Sunagawa K, and Sugimachi M.** Vagal stimulation suppresses ischemia-induced myocardial interstitial norepinephrine release. *Life Sci* 78: 882–887, 2006.
14. **Kawada T, Yamazaki T, Akiyama T, Sato T, Shishido T, Inagaki M, Takaki H, Sugimachi M, and Sunagawa K.** Differential acetylcholine release mechanisms in the ischemic and non-ischemic myocardium. *J Mol Cell Cardiol* 32: 405–414, 2000.
15. **Kawada T, Yamazaki T, Akiyama T, Shishido T, Inagaki M, Uemura K, Miyamoto T, Sugimachi M, Takaki H, and Sunagawa K.** In vivo assessment of acetylcholine-releasing function at cardiac vagal nerve terminals. *Am J Physiol Heart Circ Physiol* 281: H139–H145, 2001.
16. **Kimura J, Watano T, Kawahara M, Sakai E, and Yatabe J.** Direction-independent block of bi-directional Na^+/Ca^{2+} exchange current by KB-R7943 in guinea-ping cardiac myocytes. *Br J Pharmacol* 128: 969–974, 1999.
17. **Kimura S, Mieno H, Tamaki K, Inoue M, and Chayama K.** Nonselective cation channel as a Ca^{2+} influx pathway in pepsinogen-secreting cells of bullfrog esophagus. *Am J Physiol Gastrointest Liver Physiol* 281: G333–G341, 2001.
18. **Kléber AG.** Extracellular potassium accumulation in acute myocardial ischemia. *J Mol Cell Cardiol* 16: 389–394, 1984.
19. **Kurokawa J, Adachi-Akahane S, and Nagao T.** 1–5-Benzothiazepine binding domain is located on the extracellular side of the cardiac L-type Ca^{2+} channel. *Mol Pharmacol* 51: 262–268, 1997.
20. **Lazdunski M, Frelin C, and Vigne P.** The sodium/hydrogen exchange system in cardiac cells: its biochemical and pharmacological properties and its role in regulating internal concentrations of sodium and internal pH. *J Mol Cell Cardiol* 17: 1029–1042, 1985.
21. **Lee C, Dhalla NS, and Hryshko LV.** Therapeutic potential of novel Na^+-Ca^{2+} exchange inhibitors in attenuating ischemia-reperfusion injury. *Can J Cardiol* 21: 509–516, 2005.
22. **Li M, Zheng C, Sato T, Kawada T, Sugimachi M, and Sunagawa K.** Vagal nerve stimulation markedly improves long-term survival after chronic heart failure in rats. *Circulation* 109: 120–124, 2004.
23. **Molderings GJ, Likungu J, and Göthert M.** N-type calcium channels control sympathetic neurotransmission in human heart atrium. *Circulation* 101: 403–407, 2000.
24. **Nicholls DG.** *Proteins, Transmitters and Synapses*. Oxford: Blackwell Science, 1994.
25. **Oka T, Sato K, Hori M, Ozaki H, and Karaki H.** Xestospongin C, a novel blocker of IP_3 receptor, attenuates the increase in cytosolic calcium level and degranulation that is induced by antigen in RBL-2H3 mast cells. *Br J Pharmacol* 135: 1959–1966, 2002.
26. **Randall A and Tsien RW.** Pharmacological dissection of multiple types of Ca^{2+} channel currents in rat cerebellar granule neurons. *J Neurosci* 15: 2995–3012, 1995.
27. **Schauerte P, Scherlag BJ, Scherlag MA, Goli S, Jackman WM, and Lazzara R.** Ventricular rate control during atrial fibrillation by cardiac parasympathetic nerve stimulation: a transvenous approach. *J Am Coll Cardiol* 34: 2043–2050, 1999.
28. **Serone AP and Angus JA.** Role of N-type calcium channels in autonomic neurotransmission in guinea-pig isolated left atria. *Br J Pharmacol* 127: 927–934, 1999.
29. **Smith AB, Motin L, Lavidis NA, and Adams DJ.** Calcium channels controlling acetylcholine release from preganglionic nerve terminals in rat autonomic ganglia. *Neuroscience* 95: 1121–1127, 2000.
30. **Verkhratsky A and Toescu EC.** Endoplasmic reticulum Ca^{2+} homeostasis and neuronal death. *J Cell Mol Med* 4: 351–361, 2003.
31. **Waterman SA.** Multiple subtypes of voltage-gated calcium channel mediate transmitter release from parasympathetic neurons in the mouse bladder. *J Neurosci* 16: 4155–4161, 1996.
32. **Wheeler DB, Randall A, and Tsien RW.** Changes in action potential duration after reliance of excitatory synaptic transmission on multiple types of Ca^{2+} channels in rat hippocampus. *J Neurosci* 16: 2226–2237, 1996.
33. **Yahagi N, Akiyama T, and Yamazaki T.** Effects of ω-conotoxin GVIA on cardiac sympathetic nerve function. *J Auton Nerv Syst* 68: 43–48, 1998.
34. **Yamazaki T, Akiyama T, Kitagawa H, Takauchi Y, Kawada T, and Sunagawa K.** A new, concise dialysis approach to assessment of cardiac sympathetic nerve terminal abnormalities. *Am J Physiol Heart Circ Physiol* 272: H1182–H1187, 1997.
35. **Yoshitomi O, Akiyama D, Hara T, Cho S, Tomiyasu S, and Sumikawa K.** Cardioprotective effects of KB-R7943, a novel inhibitor of Na^+/Ca^{2+} exchanger, on stunned myocardium in anesthetized dogs. *J Anesth* 19: 124–130, 2005.
36. **Zhang JF, Randall AD, Ellinor PT, Horne WA, Sather WA, Tanabe T, Schwarz TL, and Tsien RW.** Distinctive pharmacology and kinetics of cloned neuronal Ca^{2+} channels and their possible counterparts in mammalian CNS neurons. *Neuropharmacology* 32: 1075–1088, 1993.

JACC

Reprinted from
MAY 16, 2006
VOLUME 47, NO. 10

JOURNAL of the AMERICAN COLLEGE of CARDIOLOGY

Cellular Basis for Trigger and Maintenance of Ventricular Fibrillation in the Brugada Syndrome Model

High-Resolution Optical Mapping Study

Takeshi Aiba, MD, PHD, Wataru Shimizu, MD, PHD, Ichiro Hidaka, MS, Kazunori Uemura, MD, Takashi Noda, MD, PHD, Can Zheng, PHD, Atsunori Kamiya, MD, Masashi Inagaki, MD, Masaru Sugimachi, MD, PHD, Kenji Sunagawa, MD, PHD

ELSEVIER

Journal of the American College of Cardiology
© 2006 by the American College of Cardiology Foundation
Published by Elsevier Inc.

Vol. 47, No. 10, 2006
ISSN 0735-1097/06/$32.00
doi:10.1016/j.jacc.2005.12.064

PRECLINICAL STUDIES

Cellular Basis for Trigger and Maintenance of Ventricular Fibrillation in the Brugada Syndrome Model

High-Resolution Optical Mapping Study

Takeshi Aiba, MD, PHD,* Wataru Shimizu, MD, PHD,† Ichiro Hidaka, MS,* Kazunori Uemura, MD,* Takashi Noda, MD, PHD,* Can Zheng, PHD,* Atsunori Kamiya, MD,* Masashi Inagaki, MD,* Masaru Sugimachi, MD, PHD,* Kenji Sunagawa, MD, PHD*

Suita, Japan

OBJECTIVES We examined how repolarization and depolarization abnormalities contribute to the development of extrasystoles and subsequent ventricular fibrillation (VF) in a model of the Brugada syndrome.

BACKGROUND Repolarization and depolarization abnormalities have been considered to be mechanisms of the coved-type ST-segment elevation (Brugada-electrocardiogram [ECG]) and development of VF in the Brugada syndrome.

METHODS We used high-resolution (256 × 256) optical mapping techniques to study arterially perfused canine right ventricular wedges (n = 20) in baseline and in the Brugada-ECG produced by administration of terfenadine (5 μmol/l), pinacidil (2 μmol/l), and pilsicainide (5 μmol/l). We recorded spontaneous episodes of phase 2 re-entrant (P2R)-extrasystoles and subsequent self-terminating polymorphic ventricular tachycardia (PVT) or VF under the Brugada-ECG condition and analyzed the epicardial conduction velocity and action potential duration (APD) restitutions in each condition.

RESULTS Forty-one episodes of spontaneous P2R-extrasystoles in the Brugada-ECG were successfully mapped in 9 of 10 preparations, and 33 of them were originated from the maximum gradient of repolarization (GR_{max}: 176 ± 54 ms/mm) area in the epicardium, leading to PVT (n = 12) or VF (n = 5). The epicardial GR_{max} was not different between PVT and VF. Wave-break during the first P2R-extrasystole produced multiple wavelets in all VF cases, whereas no wave-break or wave-break followed by wave collision and termination occurred in PVT cases. Moreover, conduction velocity restitution was shifted lower and APD restitution was more variable in VF cases than in PVT cases.

CONCLUSIONS Steep repolarization gradient in the epicardium but not endocardium develops P2R-extrasystoles in the Brugada-ECG condition, which might degenerate into VF by further depolarization and repolarization abnormalities. (J Am Coll Cardiol 2006;47:2074–85)

Brugada syndrome is characterized by ST-segment elevation in the right precordial leads (V_1 to V_3) of electrocardiography (ECG) and a high incidence of ventricular fibrillation (VF) leading to sudden cardiac death (1–4). However, not all of the patients with ST-segment elevation have arrhythmic events (5,6), indicating that additional factors might contribute to development of VF. Previous studies suggest that an accentuation of transient outward potassium current (I_{to})-mediated phase 1 notch and loss of action potential (AP) dome in some areas of the right ventricular (RV) epicardium but not endocardium increases transmural dispersion of repolarization (DR), which causes the ST-segment elevation (7–11). The heterogeneous loss of AP dome in the epicardium also increases epicardial DR, and a propagation of AP dome from a site where AP dome is restored to a site where it is lost might develop a local re-excitation called a phase 2 re-entry (P2R), which triggers a circus movement re-entry in the form of VF (8,9,12). It is still unclear, however, to what extent the epicardial DR is required for development of P2R and how phase 2 re-entrant (P2R)-extrasystoles produce VF. Moreover, depolarization abnormality is thought to be one of the potent arrhythmic substrate in the Brugada syndrome (13–17), but it is not fully understood how depolarization and repolar-

From the *Department of Cardiovascular Dynamics, Research Institute, and the †Division of Cardiology, Department of Internal Medicine, National Cardiovascular Center, Suita, Japan. This work was supported by grants from Japan Cardiovascular Research Foundation (Dr. Aiba) and the Japan Foundation of Cardiovascular Research (Dr. Aiba), Health Sciences Research grants from the Ministry of Health, Labour, and Welfare (Dr. Shimizu), Research grants for Cardiovascular Diseases (15C-6) from the Ministry of Health, Labour, and Welfare (Dr. Shimizu), Japan Science and Technology Agency (Dr. Sunagawa), and a Health and Labour Sciences Research grant for research on medical devices for analyzing, supporting, and substituting the function of the human body from the Ministry of Health Labour, and Welfare of Japan (Dr. Sunagawa). Presented in part at the Scientific Session of the American Heart Association, November 7–10, 2004, and published in abstract form (Circulation 2004;110 Suppl III:III318).

Manuscript received November 10, 2005; revised manuscript received November 25, 2005, accepted December 13, 2005.